



Published in final edited form as:

Expert Rev Cardiovasc Ther. 2023 ; 21(11): 817–837. doi:10.1080/14779072.2023.2273896.

Personalized biomechanical insights in atrial fibrillation: opportunities & challenges

Åshild Telle¹, Clarissa Bargellini², Yaacoub Chahine³, Juan C. del Álamo^{2,3,4}, Nazem Akoum^{1,3}, Patrick M Boyle^{1,4,5,*}

¹Department of Bioengineering, University of Washington, Seattle, WA, USA

²Department of Mechanical Engineering, University of Washington, Seattle, WA, USA

³Division of Cardiology, University of Washington, Seattle, WA, USA

⁴Center for Cardiovascular Biology, University of Washington, Seattle, WA, USA

⁵Institute for Stem Cell and Regenerative Medicine, University of Washington, Seattle, WA, USA

Abstract

Introduction: Atrial fibrillation (AF) is an increasingly prevalent and significant worldwide health problem. Manifested as an irregular atrial electrophysiological activation, it is associated with many serious health complications. AF affects the biomechanical function of the heart as contraction follows the electrical activation, subsequently leading to reduced blood flow. The underlying mechanisms behind AF are not fully understood, but it is known that AF is highly correlated with the presence of atrial fibrosis, and with a manifold increase in risk of stroke.

Areas Covered: In this review, we focus on biomechanical aspects in atrial fibrillation, current and emerging use of clinical images, and personalized computational models. We also discuss how these can be used to provide patient-specific care.

Expert Opinion: Understanding the connection between atrial fibrillation and atrial remodeling might lead to valuable understanding of stroke and heart failure pathophysiology. Established and emerging imaging modalities can bring us closer to this understanding, especially with continued advancements in processing accuracy, reproducibility, and clinical relevance of the associated technologies. Computational models of cardiac electromechanics can be used to glean additional insights on the roles of AF and remodeling in heart function.

Plain Language Summary:

People with atrial fibrillation (AF) experience a fast, chaotic heartbeat. AF greatly increases the risk of stroke. The hearts of AF patients often have an accumulation of fibrous tissue (fibrosis). Fibrosis patterns can be detected via medical imaging scans, like MRI. These images can be used to build patient-specific digital representations. These models can be used to explore how fibrosis

*Corresponding author: Patrick M Boyle, pmjboyle@uw.edu; phone: (206) 685-1392; 3720 15th Ave NE, UW Bioengineering Box 355061, Seattle, WA 98195, USA.

Reviewer disclosures:

Peer reviewers on this manuscript have no relevant financial relationships or otherwise to disclose.

might cause AF, stroke, and other health risks. Insights from imaging and modeling are becoming more and more useful as tools for personalizing AF treatment.

Keywords

atrial fibrillation; atrial fibrosis; biomechanics; medical imaging; multiphysics modeling; patient-specific modeling; patient-specific care

1 Introduction

Atrial fibrillation (AF) is a growing worldwide problem, affecting millions of people each year and predicted to increase in prevalence over the next decades [1]. It is associated with a higher risk of stroke, heart failure, and other serious health complications. The prevalence of AF is correlated with age and improved survival rate with other comorbid conditions [1]. While this indirectly implies better overall healthcare in the population, we have few tools at our disposal to prevent and predict the development of AF and for treatment following AF. Moreover, the prophylaxis of AF-associated stroke is based on non-personalized risk scores of moderate accuracies [2,3].

Irregular electrical activity caused by AF directly affects atrial and ventricular contractility and reduces diastolic and systolic function (displayed schematically in Figure 1). Excitation of atrial myocytes becomes asynchronous, which also leads to an asynchronous contraction, essentially disabling effective atrial contraction. The heavily reduced contractility leads to blood stasis, especially in the left atrial appendage (LAA), increasing the risk of thrombogenesis [4,5]. Secondly, the ventricular rapid irregular pattern affects the ventricular contraction, leading to reduced stroke volume and cardiac output [6].

AF is highly correlated with physiological and structural remodeling, altering both electrical and mechanical properties of atrial tissue [7,8]. Atrial fibrotic remodeling results from myocardial loss and collagen replacement in the extracellular space and leads to increased tissue heterogeneity. This remodeling also alters the conduction velocity; combined with electrical remodeling, this increases the probability of arrhythmia initiation [8,9]. Biomechanically, fibrosis leads to reduced contractility and altered mechanical properties (such as stiffness and elasticity) [10]. Both electrophysiological and biomechanical aspects contribute to electromechanical feedback mechanisms that can lead to prolonged, permanent remodeling. Structural changes usually precede AF – in a heart with no fibrotic structures, a patient is unlikely to develop AF. However, AF might lead to further remodeling, creating dangerous feedback loops. AF also leads to ventricular remodeling [11,12], which subsequently affects the ventricular function.

AF is often looked at from electrophysiological [8,13], pathological [14,15], or clinical [16,17] points of view. While these are important aspects of our collective understanding of AF, we here aim to focus on biomechanical aspects. The review is organized as follows: We first describe the physiological aspects of AF and how these are believed to impact biomechanical function. We next review four image-based ways of assessing the presence of atrial fibrosis, as well as four-dimensional (4D) flow magnetic resonance imaging

(MRI), used for imaging blood flow. Next, we discuss the development of representative computational models, which can be constructed from clinical images, focusing especially on biomechanical perspectives. Finally, we consider clinical guidelines and how image-based techniques can help guide personalized care of patients with AF. We finish the review with suggestions for advancing the field in three areas: biomechanical understanding, clinical imaging, and computational modeling.

2 Biomechanical mechanisms

2.1 AF impact on atrial function

AF is initiated due to a combination of triggers, electrical signals which can initiate arrhythmia, and the presence of various characteristics of the atria that sustain AF, referred to as substrate [8,18]. Triggers often come as rapid ectopic beats, originating from the pulmonary veins as well as various other locations in the atria [18], instead of from the sinoatrial node. Fibrotic regions create substrate, tissue that has reduced conductivity compared to healthy myocardium. AF also leads to altered calcium feedback dynamics [19], which affects contraction patterns. Additionally, incessant excitation does not allow the individual cardiomyocytes enough time to return to their stress-free resting state. When a new contraction is initiated while the cells are still recovering from a prior contraction, the potential active tension each myocyte can generate is heavily reduced. While fibrotic remodeling plays a central role in the pathophysiology of AF, even in patients with what used to be referred to as “lone AF” [20], there is a high degree of variability in the amount, pattern, and distribution of fibrosis between individuals. Moreover, fibrosis is a cumulative, multifactorial, slow-progressing process that generally but imperfectly correlates with the clinical pattern of AF, i.e., paroxysmal vs persistent phenotypes. The dynamics of initiation and sustenance of individual episodes of AF is also dependent on extrinsic factors (neurohormonal) and intrinsic electrophysiological atrial factors [21].

The reduced contractility subsequently affects the blood flow. In addition to acting as a passive conduit allowing pulmonary venous blood to return into the left ventricle, the left atrium stores the energy of the continuously returning blood during left ventricular systole and releases it during early ventricular diastole (reservoir function). Furthermore, it actively pumps blood into the left ventricle during late ventricular diastole (booster function). The combination of rapid activation, reduced contraction, and altered elasticity impairs reservoir and booster function, subsequently impacting the ability of the left heart to pump blood to the systemic circulation. As a result of these alterations in atrial function, the clinical consequences of AF include a wide range of symptoms including palpitations, shortness of breath, decreased exercise tolerance, and decreased energy [22,23]. These consequences have a significant impact on AF patients' quality of life. Additionally, it might promote detrimental cardiovascular endpoints including congestive heart failure with or without reduced ventricular ejection fraction [24,25], and thromboembolic phenomena including stroke.

Stroke is a leading cause of death and permanent disability worldwide [26]. Many strokes are caused by thrombi that form in the heart and embolize to occlude downstream arteries, typically in the intracranial domain [27]. The most common site of cardiac thrombosis is the

LAA. The main effects of AF on blood flow through the atrium are reduced peak velocities, increased stasis, and a limitation in atrial conduit and reservoir functions [28,29]. AF is associated with morphological changes like appendage elongation that promote LAA blood stasis and thrombosis [30–33]. These include left atrium and LAA shape, volume, flow velocity and strain rate, which all have been clinically linked to stroke risk [5]. Evidence suggests that atrial fibrosis may also play a significant role [34].

Current stroke risk assessment and mitigation paradigm is centered around population-level risk factors and comorbidities that have modest accuracy [2,3]. Shortcomings in these risk stratification tools reflect on a gap in the mechanistic understanding of cardioembolic stroke pathophysiology [34]. Structural changes due to fibrosis (leading to myocyte death, overproduction of extracellular matrix components, and alterations in myofilament alignment and/or cellular interconnectivity) usually precede AF, and can create a substrate for AF initiation and perpetuation. Persistent AF can in turn lead to additional structural remodeling of the cardiac tissue [12,35]. As such, AF and atrial fibrosis are interconnected and are increasingly studied in terms of synergistic interactions.

2.2 Calcium remodeling and its implications

Electrical remodeling, hereunder calcium remodeling, both creates substrate for AF and is a consequence of AF [7,36]. The calcium remodeling affects both intracellular and membrane subprocesses [36]. Rapid atrial and ventricular pacing in animals have revealed alterations in ion channel expression [37–39] and that the remodeling is highly spatially heterogeneous [40]. Atrial function is temporarily depressed in patients with periodic AF following restoration of sinus rhythm, believed to be mostly determined by calcium remodeling [36,41].

The calcium remodeling leads to decreased calcium transients which in turn leads to reduced contractility [41], such that the biomechanical function is reduced. Conversely, an enhanced positive force-frequency behavior has been observed in atrial cells taken from AF patients in SR compared to patients with chronic AF [42], which increases both the calcium transient and the contractile force upon rapid pacing. The enhanced force-frequency behavior might make up for some of the loss in contractility.

2.3 Fibrosis structure and implications

Fibrosis can be classified into two major categories, diffuse and replacement fibrosis [43,44] (schematically represented in Figure 1A). Diffuse fibrosis is also referred to as reactive fibrosis, and replacement fibrosis as focal or reparative fibrosis. Diffuse fibrosis might be further classified as interstitial fibrosis, developing in the cardiac interstitium, and perivascular fibrosis, progressing around blood vessels [45,46]. Interstitial fibrosis can also be more accurately described as endomyxial or perimyxial, depending on whether it develops between cardiomyocytes or myocardial bundles [15,44,47]. Finally, infiltrative fibrosis is a rare form for fibrosis in which non-matrix material accumulates in the extracellular space [44]. Infiltrative fibrosis has many common traits with diffuse fibrosis, especially as it progresses by expanding the space between cells rather than leading to myocyte death. Replacement fibrosis can further be classified as *compact* or *patchy*, depending on the

way it progresses. Patchy fibrosis is associated with greater arrhythmia risk than compact fibrosis [48]. Fibrosis classifications are quite descriptive and qualitative, based on patterns commonly observed rather than on specific underlying molecular or cellular development mechanisms. One type of fibrosis rarely occurs in isolation; within the same tissue, one can usually observe multiple variants.

Diffuse fibrosis is characterized by an expansion of the extracellular space around the cells. Atrial diffuse fibrosis might develop due to irregular stress over time because of factors such as pressure overload [49]. In animal models of permanent AF, endomyocardial fibrosis is prevalent while the perimysium remains unaffected [47]. Cells are not replaced in diffuse fibrosis – instead, the matrix surrounding them expands. However, if the stressors are not mitigated they can eventually lead to cardiomyocyte death and replacement fibrosis [50]. As the interstitial space expands, the relative density of force-producing myocytes versus matrix space decreases, leading to reduced contractility, negatively impacting the various atrial functions described above. Diffuse fibrosis often develops gradually over time. However, rapid ventricular tachycardiomyopathy can also cause tissue stiffening [51], indicating that structural remodeling (alike to changes in calcium handling) can also be induced by sudden changes in heart rhythm.

Replacement fibrosis occurs when lost cardiomyocytes are replaced by fibrotic tissue. Atrial replacement fibrosis commonly occurs after infarction or injury from catheter ablation, but it can also be the long-term consequence of untreated diffuse fibrosis. Replacement fibrosis constitutes a part of a healing or reparative process in which new collagenous matrix partially restores tissue integrity and function [15]. Various sub-mechanisms are involved in this process [44], including fibroblast activation and differentiation into myofibroblasts. Myofibroblasts are more efficient in extracellular matrix component production and contribute to a quick healing process. The damaged area is replaced by collagenous, non-contracting tissue. The main biomechanical implication is that the affected part of the tissue no longer contributes to the generation of contractile force.

Structural changes due to fibrosis lead to changes in the tissue's mechanical properties. Healthy cardiac tissue is significantly stiffer along the myocyte longitudinal direction than in the transverse directions. Analogously collagen alignment is important for relative anisotropy in infarcted tissue, varying on a smaller scale than myofiber alignment. Collagen is the main component of mature scar, with at least a two-fold increase in crosslinking compared to in healthy tissue [52]. Infarcted ventricular tissue from animal models have been found to be both mechanically anisotropic [30,53–55] and isotropic [56,57], overall consistent with whether or not the collagen fibers were aligned. Holmes et al. found that circumferential strain decreased compared to healthy ventricular myocardium, while longitudinal and radial strains were comparable [53], and Sirry et al. found that circumferential stiffness increased significantly more than longitudinal stiffness [54]. It is likely that it is most beneficial, in terms of being least disruptive to the cardiac function, if the collagen fiber direction is overall consistent with the original myofiber direction in fibrotic areas.

Collagen is not the only determinant of myocardial stiffness. Non-myocyte cells such as fibroblasts and myofibroblasts also contribute – their stiffness properties, geometries, alignment, and interconnectivity all impact the tissue’s stiffness and elasticity. Cell-cell junctions, which interconnect myocytes electrically and mechanically, are hypothesized to also connect myocytes to non-myocytes. These connections may play a role in arrhythmia development, but this process remains poorly understood [48,58]. Additional experimental work and detailed microscale histological images, from which relative structures and dimensions can be derived, might lead to additional insights of the individual contributions.

2.4 Feedback mechanisms

Atrial remodeling and AF often occur together. The presence of one is known to increase the risk for the other through complex feedback mechanisms not yet fully understood [59,60]. Electrical and fibrotic atrial remodeling are both important factors in AF development, as they introduce tissue heterogeneities. Likewise, it is also likely the presence of AF itself causes additional electrical and structural remodeling.

Several electromechanical feedback mechanisms may contribute to the joint development of AF and atrial fibrosis, including stretch-induced remodeling [61], inflammation [62], and neurohormonal activation [63]. Of note from a biomechanical point of view, stretching of myocytes, fibroblasts, and increased matrix stiffening can all lead to fibroblast activation [64]. Stretching around the pulmonary vein (e.g. caused by increased hemodynamic pressure) also increases the risk of spontaneous ectopic beats [65,66] as well as calcium sparks and waves [36].

Changes in flow and structural remodeling are also correlated. Disrupted flow-stresses due to chronic blood flow disturbances promote vascular remodeling as an adaptive response for maintaining homeostasis. For instance, irregular oscillatory endothelial shear stresses and pressures in the endocardium can lead to structural remodeling as a homeostatic response aiming to restoring normal shear stress and wall tension. In turn, such remodeling is responsible for the perpetuation of pathophysiological stresses, initiating a feedback loop that promotes disease progression [67–69].

AF and structural changes are unique for each patient. There is inter-individual variability in atrial geometry and AF development, in which the above-described mechanisms might progress in different ways over time. Some characteristics are recognized statistically, e.g., by differences in atrial wall thickness [70] and ion channel expression [71]. Others vary widely, such as the spatial pattern of fibrosis progression. Recognizing common patterns in how fibrosis and AF emerge on a personalized basis might be important for improving risk stratification and personalized treatment plans.

3. Clinical imaging techniques and applications

Clinical imaging is used to assess the cardiac function, differences in anatomical shape, and spatial patterns of fibrosis progression. Atrial fibrosis detection is used in the diagnosis of several diseases, but also provides a valuable research tool to improve our understanding of the relationship between atrial remodeling and AF progression. In addition, clinical images

are fundamental inputs for personalized computational modeling and simulation, which can be used to better understand underlying mechanisms in AF and how AF contributes to the hemodynamic substrate for ischemic stroke. In this section, we review and compare four clinical imaging methods for fibrosis detection – late gadolinium enhancement (LGE), T₁ mapping, strain, and elastography. Differences and similarities between the different methods are highlighted in Table 1. We also review how 4D flow MRI could potentially be used to derive clinically relevant metrics based on blood flow rather than fibrosis patterns.

3.1 Late gadolinium enhancement

LGE is the most widely used technique for *in vivo* fibrosis detection and is particularly well suited for detecting replacement fibrosis [79]. In LGE, MRI is used to image the heart after the injection of gadolinium, a contrast agent that can help reveal fibrotic areas. The method has been verified histologically, both in animal models and through biopsy [80,81]. The procedure is common in many clinical centers with acceptable associated costs [82]. However, it remains too costly to be established as a standard-of-care procedure in low- and middle-income countries, motivating exploration of more cost-efficient pipelines [83].

LGE quantification is carried out via voxel intensity thresholding. The specific thresholds vary between different underlying methods. Harrison et al. [80] considered signal intensity thresholds for ablated ovine hearts and found 2.3 standard deviations (SD) to be most accurate acutely, and 3.3 SD most accurate chronically post-ablation. Hopman et al. [84] compared two different methods, image intensity ratio (IIR) and 3 SD (using two different software) and found that one-third of the patients were classified into different categories in the Utah classification system based on methodological differences only [84]. Boyle et al. [85] compared pixel intensity histogram (PIH) and IIR across different thresholds, in which they found the results to vary significantly and that PIH was a better predictor of AF than IIR. However, it remains unclear how these differences emerge, and further studies are needed to explain the underlying reasons. The PIH method was used in the multi-center studies DECAAF [86] and DECAAF-II [87], whereas the IIR method was used in the ALICIA study [88]. These and other studies have demonstrated the feasibility of the approach in tens of sites. However, wide scale adoption has been challenging due to the required expertise in good-quality image acquisition and the absence of a gold standard in image processing.

An alternative to thresholding, which classifies tissue as fibrotic or non-fibrotic in a binary way, is to grade fibrosis using several intensity levels. Benito et al. [89] used different thresholds to classify fibrosis as “dense” or “overall”, suggesting that these correspond to replacement fibrosis (scar) and interstitial fibrosis, respectively. Risk assessment scores could also be assigned based on spatial patterns above percentage. Patchy fibrosis is more arrhythmogenic than compact fibrosis [48], so it might be meaningful to develop metrics that take such aspects into account. Artificial intelligence-based methods are also explored as options to existing image segmentation tools [90] and might eventually be integrated also in clinical settings. Furthermore, fibrosis has histologically been correlated with reduced conduction velocity [91,92]. If a mapping is established between different levels of fibrosis and corresponding expected reduction in conduction velocity, electroanatomical mapping

could potentially be used in combination with LGE to help establish more consistent threshold values.

3.2 T₁ values

The use of T₁ values is emerging as an alternative technique to LGE for detection of fibrotic patterns. Validation of novel metrics based on T₁ and T₂(*) values are expected to increase accuracy, sensitivity, and diagnosis confidence in general, among which T₁ values are best suited for detecting myocardial fibrosis [93,94]. Intensity metrics are reported as absolute values based on contrast clearing rates in the MRI images, making T₁ values more suitable than LGE for detecting diffuse fibrosis [44].

Elsafty et al. [94] compared contrast-free T₁ assessment and LGE in the ventricles, considering patients with various cardiac conditions. They found results based on LGE and T₁ values largely comparable, however T₁ values were significantly higher than normal also for areas not detected as fibrotic by LGE in hypertrophic myopathy and dilated myopathy patients. Atrial T₁ transients are shorter in patients with paroxysmal and persistent AF than among healthy volunteers, in which shorter T₁ transients regionally correspond to areas of reduced voltage [72,73] and are overall negatively correlated with fibroblast growth factor levels [76]. Bouazizi et al. [95] performed histology comparison to T₁ mapping *ex vivo* on left atrial tissue, correlating the values to areas containing diffuse fibrosis, fat, or the combination of both.

As T₁ values are calculated absolutely, they can be compared to reference values obtained from healthy volunteers. Reference numbers are reported differently depending on the strength of the magnetic field [96] and the sequence used to obtain the images [97,98]. For the left ventricle in healthy volunteers, T₁ values differ depending on sex, age, and myocardial segment [96,99]. These dependencies are likely to exist for atrial values as well. In the absence of more specific values for atrial tissue, representative average T₁ values are commonly used. Values used for normal atrial tissue are lower than normal ventricular values, broadly specified in a range around 250–500 ms [72,73] (compared to ventricular values 950–1200 ms [100,101]).

3.3 Strain imaging

Cardiac contraction can be characterized by tracking visible motion of the heart in clinical imaging. Motion is commonly recorded using either echocardiography or the costlier but more accurate Cine-MRI [102]. From motion measurements, one can derive strain, which quantifies local deformation. Strain-derived metrics are correlated with fibrosis as detected by LGE [74,103], native T₁ values [76], and histology [75,104].

Strain is mathematically derived by differentiating the cardiac displacement field along different directions. Motion quantification can be performed via techniques like Tissue Doppler Imaging (TDI) and Speckle-Tracking Echocardiography (STE); strain is next derived from the motion [105–107]. In clinical settings, atrial strain is usually either assessed region-by-region [103] or as relative shortening and expansion across the atrium [74,108]. A time-dependent transient is derived from the strain values, usually displayed over one cardiac cycle. Depending on the software used, this transient either starts at the

beginning of the P wave or at the beginning of the QRS complex [31,107]. Different parts of the transient quantify strain during the reservoir, conduit, and contractile phases (see Figure 2) [74,107]. The peak atrial longitudinal strain (PALS; i.e., strain at the end of the reservoir phase) and peak atrial contractile strain (PACS; i.e., strain at the end of the atrial contraction phase) are commonly used metrics of atrial function [107].

Several studies have investigated the correlation between strain and AF and/or atrial fibrosis. Hopman et al. demonstrated that AF patients had significantly reduced PALS and PACS compared to healthy controls, and that high levels of LGE-assessed fibrosis were correlated with reductions in PALS, but that PACS was unaffected [74]. Lisi et al. showed that, in heart failure patients, a high degree of fibrosis as determined by post-transplant histology was correlated with lower PALS [75]. Çoteli et al. reported a negative correlation between T_1 contrast clearing rate and PACS [76]. Kim et al. found that PALS could predict the presence of fibrosis in the LAA, correlated with the risk of AF recurrence following ablation [104]. Overall, the presence of AF and/or atrial fibrosis is expected reduce strain, but more studies are needed to establish how these metrics can be used in clinical settings.

Strain metrics provide important biomechanical biomarkers, but they also come with limitations. Strain measurements integrate many factors, not only effects from the extent and pattern of fibrosis but also many other independent clinical factors correlated with left atrial strain [107]. For patients in AF at the time of image acquisition, atrial strain imaging is challenging and might not be meaningful. Strain measurement is sensitive to image resolution [109], which is a bigger problem for atrial than for ventricular imaging due to differences in wall thickness. An advantage of atrial strain imaging compared to LGE is that it does not require contrast. Strain measurement can be performed serially, including for patients with no signs of AF, which makes it a more attractive approach for preventive care applications.

3.4 Myocardial elastography

Myocardial elastography can quantify the elasticity of cardiac tissue *in vivo*, from which the stiffness can be derived. Elastography is routinely used clinically to detect liver fibrosis but is still only used experimentally in cardiac imaging. The procedure is performed by mechanically exciting the tissue, measuring the local vibration response. Stiffness values are then derived based on equations describing the relation between strain and force [110]. Diseased (e.g., fibrotic) tissue has different elastic properties than healthy myocardium. Left atrial stiffness estimated indirectly from strain is independently associated with AF recurrence after radiofrequency catheter ablation [111]. More direct measurements of cardiac stiffness (e.g., via elastography) could potentially give rise to more sensitive and specific metrics to be used in clinical decision-making [112][110]. However, elastography requires special equipment and is considered costly [112] which currently might limit potential usage.

There are two main elastography techniques: magnetic resonance elastography (MRE) [113] and ultrasound-based shear wave elastography (SWE) [114]. MRE is more suitable for non-invasive measurements since ultrasound has limited penetration depth [112]. Both methods capture increased myocardial stiffness among patients in which increased stiffness is

expected [43,115–118]. There is correlation between age and shear wave velocity (indirectly measuring myocardial stiffness) in healthy volunteers [116,118], likely due to age-related fibrosis deposition. Regions with higher stiffness as measured by elastography correlate with fibrotic regions delineated by LGE [43]. Elastography has also been used to quantify stiffness and visualize atrial ablation lesions in animals [119–122], including in real-time during the ablation procedure [122], and in patients [123,124].

Myocardial stiffness depends non-linearly on local stretch, which varies across different cardiac regions, time phases in the cardiac cycle, and depends on local myofiber alignment [112]. This makes acquiring mechanical measurements from cardiac muscle more complicated than for many other organs, but also provides new avenues for assessing cardiac variables of interest. For instance, Couade et al. used SWE in sheep hearts to characterize time-dependent stiffness variation over the cardiac cycle and transmural anisotropy [125]; Mazumder et al. combined diffusion tensor imaging with MRE elastography to find the myofiber alignment and derive locally defined anisotropic stiffness values [126]; and Villemain et al. found that tissue anisotropy was higher among healthy volunteers than among patients with hypertrophic cardiomyopathy [116]. Miller et al. used elastography data to estimate material parameters of cardiac tissue by solving an inverse problem [127], demonstrating the feasibility of personalizing material parameters.

Most studies on cardiac elastography have been carried out focusing on ventricular tissue, and there are several additional aspects that need to be considered moving over to the atria. Myofiber structure is more complex in the atria compared to the ventricles [128]; as such, atrial elastography might require finer-scale segmentation methods. Geometrical challenges are also relevant because the thinness of atrial walls compared to the ventricles demands higher resolution imaging.

3.5 4D flow MRI

Thromboembolic risk in AF patients is partly due to reduced blood flow, especially in the LAA [129,130]. Phase contrast techniques that facilitate flow mapping in the heart, such as 4D flow MRI (i.e., 3D time-resolved), hold potential to help explain hemodynamic causes of thromboembolism in AF [29,131]. Compared to other imaging techniques like Doppler transesophageal echocardiography (TEE), 4D flow MRI offers time-resolved, 3D blood flow evaluation with full coverage of the left atrial and LAA. Markl et al. [29] and Costello et al. [132] have suggested that this technique can be used in AF patients to quantify hemodynamic measures like peak flow velocity and blood stasis (residence time), characterize atrial hemodynamic patterns, and predict risk of ischemic stroke. This analysis could also be carried out between AF cohorts with different types of fibrotic remodeling to better understand relationships between fibrosis, AF, and stroke [133].

Information obtained with 4D flow MRI can be combined with LGE, T_1 values, and/or strain imaging, to gain a more comprehensive characterization of cardiac pathologies. This has already been attempted in several ventricular studies, studying pulmonary hypertension [134], hypertrophic cardiomyopathy [134], and left-sided valvular heart disease [135]. In the context of AF, this approach could (as suggested above) be applied to cohorts with different fibrosis patterns or assessed in conjunction with contractility patterns (e.g. strain

rate) to understand effects of structural factors on flow and vice-versa. This will allow a more exhaustive overview of the factors leading to and characterizing AF.

Despite the many potential opportunities outlined above, 4D flow MRI also has limitations. Although evaluation of advanced flow parameters is possible and constantly improving, measurement of these metrics can be sensitive to artifacts (i.e., image noise), dependent on spatiotemporal resolution, or complex to implement in practice. Moreover, the imaging technique relies on reconstruction and post-processing methods. These can allow noise propagation and systematic errors, and it impose clinically relevant limits on the spatial and temporal resolutions of images acquired [136,137].

4 Computational modeling opportunities

Computational models enable the exploration of mechanisms that cannot be evaluated clinically or through physical experiments. In clinical and experimental settings, phenomena of interest occur together simultaneously, interact, and are difficult to disentangle; in computational models, simulated physiological effects and their underlying driving factors can be manipulated directly, independently, and safely. To date, computational models have most commonly been used to decipher underlying mechanisms, but they are also emerging as useful tools to guide clinical decisions [138,139].

4.1 Fundamental modeling principles

Computational models are created from symbolic equations describing physical laws within and between different subsystems involved. The models are parameterized and validated through experimental and clinical data. When applied to geometric domains representative of heart tissue and discretized in time and space, these models give rise to systems of up to billions of arithmetic equations. Numerical solutions of the latter can be computed to simulate specific aspects of cardiac physiology. Simulation outputs can reasonably be interpreted as predictions of the heart's behavior given the laws of physics and any imposed constraints, with the caveat that all models simplify real-world physiology. Computational models can only be as realistic as the information used in their parameterization, and combining them with suitable data (e.g., from clinical imaging, experimental measurements, etc.) is crucial in terms of creating physiologically realistic models.

Mechanistic cardiac models are commonly built on laws from one or more of three physical branches: electrophysiology, biomechanics (solid mechanics of the myocardium), and hemodynamics (cardiovascular models). Single-physics models are useful since they facilitate deep exploration of research questions in the absence of potential confounding factors. However, we know the different physical aspects of cardiac physiology are interconnected, which motivates coupling them through known pathways; see Figure 3. Multi-physics coupling in cardiac simulations is usually performed by linking electrophysiology with biomechanics, and/or biomechanics with fluid mechanics. Many challenges are associated with this process, for example the fact that the relevant aspects of cardiac electromechanics and blood flow occur in non-overlapping domains (i.e., within the myocardial wall vs. within the heart's chambers), which complicates the implementation of computational models. Other major challenges include model construction and validation,

efficiency of numerical solvers on high-performance computing systems, and lack of fully developed software [140].

Pure electrophysiological models typically integrate ion channel dynamics and cell-level dynamics with propagation of the electrical signal at the tissue and organ scales [141,142]. They can be directly connected to biomechanical models through the dynamics of intracellular calcium transients, working on the myofilament level [143], and indirectly (capturing feedback mechanisms) through stretch-activated ion channels [144]. At the tissue and organ scale, biomechanical models represent myocardial kinematics derived from laws of solid mechanics [145]. These equations describe myocardial contraction based on equations connecting stress and strain patterns. Biomechanical models can be coupled with hemodynamic models either through compartment models of the circulation or spatially resolved flow models. These mechanofluidic models capture the interactions between intracavitary blood pressure and myocardial kinematics [146]. Hemodynamic models can also be created without the biomechanical coupling, either using stationary geometries or by prescribing myocardial wall motion based on time-resolved CT or MRI images [147]. These spatially resolved flow models describe the internal blood flow via the Navier-Stokes equations governing fluid dynamics [147]. All these models capture different parts of cardiac dynamics, as described by mathematical equations.

These governing equations are combined with geometric representations of the heart (or parts thereof) to create 3D organ-scale representations. These geometric representations are derived using custom software [148–150] and can be representative, with dimensions and attributes matching generic human features [151–153], or patient-specific (i.e., personalized) derived from individual clinical imaging scans [154–156]. Myofiber direction is a key parameter in both electrophysiological and mechanical simulations since it gives rise to anisotropic properties of conduction and contraction. To represent this aspect, each cardiac geometry is associated with a map of myofiber orientations. Since standard clinical imaging cannot resolve myofiber orientations, the current community standard is to map a generic fiber distribution into each patient-specific geometry [157–160]. Beyond cardiac anatomy, biomechanical aspects of patient-specific computational simulations can often be further personalized with appropriate clinical data, like strain measurements or spatial fibrosis distributions (see Table 2). In some cases, multiple scans from an individual patient are combined in order to capture multiple clinical aspects (e.g., pre- and post-ablation LGE-MRI to capture procedure-created scar and residual fibrosis [173]; T₁-weighted imaging and LGE used in combination to derive a representation of both dense and diffuse fibrosis [174]).

4.2 Modeling mechanical properties of atrial tissue

Mechanical modeling of cardiac tissue balances contributions from active tension (generated by myocytes) and passive tension (determined by myocardial elasticity properties). The myocardium is often modeled as a spatially defined mechanical continuum [145], in which displacement, strain, and stress are dictated by the equilibrium of forces. Cell-level dynamics are more commonly described via time-dependent equations describing different statistical states, not necessarily spatially resolved [175].

Myocyte contraction is typically modeled by representing myofilament crossbridge cycling prompted by transient increases in intracellular calcium [176,177]. Atrial contraction is faster than ventricular contraction, which is physiologically explained by the abundance of α -myosin in human atrial myocytes (whereas β -myosin is dominant in ventricular cells) [178,179]. For electromechanical modeling of the atria, these faster contractility rates have been represented by calibrating existing ventricular myofilament models to match data from atrial myocyte experiments [180–184].

Representation of altered contractility due to AF and/or fibrosis in computational models strikes a balance between multiple complex aspects and remains an area of active research. The relative levels of myosin isoforms in atrial cells from AF patients are disrupted compared to healthy controls [185], suggesting they may contract and relax more slowly. Consequences of this finding have not yet been explored computationally, but might feasibly be incorporated in organ-level models via myofilament models [179]. Effects of AF on biomechanics can otherwise be imposed indirectly by increasing the rate of electrical pacing [171,186] or modifying ion channel expressions and/or gap junction-mediated conductivity to reflect AF- or fibrosis-related remodeling [186,187]. Electromechanical models can capture how these alterations in electrical properties via calcium lead to reduced contraction [181,186] (see also Figure 4B). Zile et al. [183] showed (using a cell-scale model) that when the mechanical component was included, action potential duration alternans were dampened due to the role of calcium in feedback mechanisms. In a more recent model, Mazhar et al. [184] captured a positive force-frequency relationship both for calcium and for contraction force. In isolation, the positive force-frequency behavior would be expected to increase cell-scale contractility during rapid AF rhythms, possibly restoring some amount of the reduced contractility. However, to our knowledge, this question remains unexplored in organ-scale models. Contractility is also reduced in fibrotic tissue due to the reduced number of force-producing myocytes; thus, reducing or removing contractility in fibrotic regions may be helpful for representing fibrosis; as done by Phung et al. in their model of ablated tissue [188]. In reality, physiological contractility reduction is the consequence of multiple interacting factors – a future application of computational models may be determining their relative importance.

The passive tension arises from the tissue's mechanical properties, which are known to be non-linear and anisotropic [171]. Relationships between stiffness and deformation are often described through strain energy functions [145], parameterized through deformation experiments along different directions and for different levels of stretch. There is significant variation in parameter values as reported in literature, even considering healthy ventricular tissue [189]. Stress-strain experiments have also been performed on atrial tissue to quantify its mechanical properties [51,190–192], notably finding that it is softer and less anisotropic than ventricular tissue [192].

Fibrosis alters tissue stiffness and anisotropy, which can be adjusted in computational models. Moyer et al. modeled atrial fibrotic tissue by increasing the isotropic shear stiffness while leaving the anisotropic contribution unchanged [171]; in other studies, ablated tissue has been modeled by increasing the isotropic component and removing the anisotropic component [170,188]. Experimental data are mostly based on infarcted ventricular tissue

from animal models and quantification values vary significantly [54–56,193,194], often found to be consistent with the collagen fiber alignment. Some combined experimental/computational studies suggest explicitly including this collagen fiber disparity in the model [55,193,194]. While certainly comparable, infarcted ventricular tissue is not the same as fibrotic atrial tissue, and more accurate models could be developed by performing stress-strain experiments targeting this explicitly.

Clinical imaging techniques hold promise in acquiring patient-specific spatial patterns of fibrosis and material properties of atrial tissue with varying degrees of fibrosis. In the context of computational modeling, LGE and T_1 values are particularly well suited for detection of spatial patterns. Elastography might help determine personalized values for both healthy [127] and fibrotic myocardium, which could replace the nominal values currently used, leading to more representative models. For accurate representation of the active tension, electrocardiogram (ECG) or invasive electroanatomical mapping (widely used in electrophysiological models [138]) or more recent methods like electromechanical wave imaging [195,196] could be used to ensure accurate representation of the electrical signal in coupled electromechanical models, leading to more accurate representations of contraction timing.

4.3 Take-aways from organ-scale biomechanical models of AF

Cardiac electrophysiology has been explored computationally for decades, with AF mechanisms as a major focal point [138,197]. While less extensively studied than electrophysiology, there are also mechanical models for the atria. Some are purely mechanical [161,198], some are electromechanical [167,180,186,199,200], some are mechanofluidic [165,171,188], and some are multiphysics models taking all three aspects into account [164]. Atrial mechanical models are also a subset of whole-heart [162,163,166,168–170,201–203] and left-heart models [204,205].

Some of the biomechanical computational studies cited above focused explicitly on AF. Hunter et al. [161] used a purely biomechanical (single-physics) model to investigate stress distributions considering 20 patients undergoing ablation for persistent AF, with geometries constructed from computed tomography (CT) scans. Their model predicted that stress distributions varied within the atria and between subjects and that areas with high stress were associated with low voltage. Moyer et al. [171] used a biomechanical model coupled with a 0D circulatory model, and constructed a representative left atrial geometry from MRI data then explored how different biomechanical features impacted the cardiac function and compared model predictions to clinical data. Dilation, increased pressure, and the presence of fibrosis were found to explain most of the biomechanical differences between the healthy volunteers and AF patients. Adeniran et al. [186] used a bi-atrial model reconstructed from the Visible Female dataset to examine the consequences of imposing AF-induced electrophysiological remodeling. They showed that atrial contractility was greatly reduced at sinus rhythm-like heart rates and practically eliminated in the context of rates consistent with AF (see Figure 4). Feng et al. [165] developed a coupled mechanofluidic model, with a spatially resolved flow field, and represented AF by total removal of active contraction. Their simulations predict that AF eliminates flow reversal in the pulmonary veins during late

diastole and may impair LAA filling during systole. They also noted that their simulation results were sensitive to geometric properties of the atria; specifically, thicker walls in the appendage led to reduced blood flow velocity.

Lastly, many computational biomechanics studies have indirectly explored AF-related questions. Some have explored the potential impact of catheter ablation on cardiac function has been assessed via simulations [164,170,188]. These models considered how ablation-induced stiffening and contractility impairment impacted systolic and diastolic atrial function depending on the lesion set strategy used to abolish AF inducibility. They found that ablation of areas with high motion was more consequential for atrial function in terms of blood flow. Complementary electrophysiological modeling studies have also explored optimization of AF ablation [206,207], highlighting how simulations can be used to optimize the lesion set required to neutralize fibrotic substrate or minimize the amount of isolated myocardium. Other biomechanical models, while not incorporating AF directly, have been used to study how genetic variability of ion channel expression in AF patients impact contractility [199], the relation between strain and areas in which triggers are likely to occur [200], and how stress distributions depend on wall thickness [167]. These factors are difficult or impossible to control clinically, but computational models can help build an understanding of how they may be mechanistically linked to AF disease development and/or symptom severity.

4.4 Spatially resolved hemodynamic models

Spatially resolved flow models describe the blood flow via the Navier-Stokes equations governing fluid dynamics [147]. Post-processing of spatiotemporally resolved flow fields allows for delineation of stagnant blood volumes and areas of disturbed endocardial shear stress, where thrombosis is more likely [208,209]. Hemodynamic models can be extended by coupling fluid motion with the reaction kinetics of the coagulation cascade [210–212]. Such chemo-elasto-fluidic descriptions can link myocardial biomechanics with the concentration of pro-coagulatory enzymes like thrombin. These approaches have translational promise, given the growing availability of pharmacological agents targeting different stages of the coagulation cascade (e.g., factor X vs. factor XI) [213]. However, spatially resolved chemo-elasto-fluidic models are complex and costly. A common simplification is to constrain computational fluid dynamics (CFD) solvers of the Navier-Stokes equations with atrial chamber segmentations from medical imaging, and use blood stasis metrics as surrogate indices of clotting risk [214–220].

Among spatially resolved flow models, the more sophisticated variants represent AF via removal of active contraction [165,221] or use of high-resolution 4D images from AF patients [218,222]. A less involved approach is to perform simulations on stationary anatomies with modified flow boundary conditions that mimic the absence of atrial contraction (a.k.a. fixed-wall simulations). Findings from stationary anatomy simulations vary, and caution must be exercised when comparing models of differing fidelity (e.g., moving walls vs. fixed walls, Newtonian vs. non-Newtonian blood viscosity) and the geometric resolution of computational representations [218,219,223]. Nevertheless, the emerging picture is that atrial function influences blood stasis in a manner that is sensitive

to patient-specific factors like LAA shape, ostium area, pulmonary vein configuration, hematocrit levels, and even postural changes [165,215,216,218–221,224–236]. Overall, the use of patient-specific atrial flow models is expected to pave the way towards improved understanding of the mechanisms underlying AF and thrombus formation, including their relationship to atrial fibrosis.

4.5 Combined use of statistical and mechanistic models

Computational models can be broadly subclassified as mechanistic (reviewed above) and statistical (i.e. artificial intelligence/machine learning) models. Mechanistic models are based upon physical laws and principles while statistical models exploit our understanding of predictable patterns. Statistical models are often utility-driven (e.g., predicting the occurrence of events like AF [237] or stroke [238]) while mechanistic models focus on explaining underlying mechanistic patterns. Combined with relevant clinical images for the atria, such as LGE [239–241] and strain [242], statistical models can be strong predictors. Challenges have been launched where groups use the same clinical data to train, validate, and test predictive models [243,244], creating a useful basis for comparing distinct approaches. In synergy with mechanistic models, statistical methods can also be predictors of variables of interest – i.e., they can identify parameters in the mechanistic models worth further exploration. Statistical models can also predict the outcomes of mechanistic simulations (in which verifying predictive accuracy can be done by completing full mechanistic runs for a subset of cases), rendering the computations more time-efficient overall [203,245]. Any such combination requires mutual evolution of the mechanistic and statistical frameworks, and in the best-case scenario the two approaches complement each other and reveal valuable new understanding.

5 Clinical care perspectives

Clinical imaging is helpful in developing AF treatment plans. LGE-guided assessment of fibrotic remodeling gives insight into patient-specific AF stages and expected outcomes from treatment strategies, especially catheter ablation. The extent of baseline (pre-ablation) LGE fibrosis is associated with poor outcomes following catheter ablation for AF [86]. Higher residual fibrosis after ablation has been significantly associated with higher postprocedural recurrence rates [246] and may create anchor points for reentry in the context of post-ablation arrhythmia recurrence [239]. In the DECAAF-II study, pulmonary vein isolation was combined with LGE-guided fibrosis ablation for substrate homogenization, but this did not significantly reduce the rate of arrhythmia recurrence in patients with persistent AF [87]. King et al. demonstrated a higher risk of stroke in patients with the highest degree of LGE-MRI fibrosis in patients with AF [247]. Similarly, strain assessment has been used to predict post-ablation AF recurrence [78,248,249] and left atrial thrombus formation in patients in sinus rhythm [250].

The relationship between atrial fibrosis and stroke seems to persist regardless of the presence of arrhythmia, as evidenced in patients with cardiac implantable devices and patients with embolic stroke of undetermined source (ESUS). Temporal dissociation between device-detected atrial arrhythmia episodes and thromboembolic events has been observed in

patients with cardiac implantable devices, with the 30 days prior to thromboembolic events being arrhythmia-free [251]. AF and ESUS patients have comparable levels of atrial fibrosis [252], and ESUS patients with high atrial fibrosis burden are at higher risk of new-onset AF or recurrent stroke [253]. Bifulco et al. demonstrated in a computational electrophysiological model study that fibrotic remodeling in patients with ESUS has the same fundamental proarrhythmic properties as it does in AF patients, prompting the hypothesis that ESUS patients with fibrotic atria may be spared from arrhythmia due to a lack of triggers [254]. The presence of atrial fibrosis might thus be a better indicator for risk assessment related to thrombus formation than AF.

Histologically quantified LAA fibrosis is higher in patients with thrombi in that area compared to those without [104,255]. The contribution of atrial fibrosis to thrombogenesis is not completely understood, but it is likely that the concomitant reduction in strain generation plays a role. Patients with AF have a higher mean blood residence time compared to patients without AF [218]. The assessment of ischemic stroke risk in AF currently relies on clinical risk scores such as CHADS₂, CHA₂DS₂-VASc, and ATRIA. However, all these scores remain imperfect predictors of stroke with modest predictive accuracy [2]. Overall, development of more fine-grained imaging techniques might lead to the development of improved metrics, giving us better stroke risk assessment tools in the future.

Being a multifaceted and heterogenous disease, AF requires structured patient management and specific treatment decisions like stroke thromboprophylaxis and symptom control. 4S-AF is a structured pathophysiological AF characterization scheme incorporating stroke risk, symptoms, the AF burden, and substrate severity; it has been proposed as a means of overcoming limitations of AF classification based on episode duration and temporal patterns alone [256]. 4S-AF includes imaging-based assessment of the atria and structural remodeling predisposing to or resulting from AF, providing new means to facilitate, improve, and personalize AF management.

Interactions between fibrotic remodeling and electrophysiological and biomechanical properties of the left atrium remain areas of active investigation. LGE fibrosis imaging has proven clinically useful in arrhythmia and stroke management, and many experimental studies suggest strain as a reliable predictive tool. The use of other imaging techniques such as T₁ mapping and elastography might give additional insights in fibrosis progression, and incorporation of information from 4D flow CT or MRI can help infer thrombosis risk. A major step towards unlocking these valuable new insights will be the development of patient-specific multi-physics, multi-scale cardiac simulations informed by improved imaging techniques. As outlined in this review, multiple recent technological developments set the stage for the research community to derive heretofore elusive mechanistic understanding of links between fibrosis, arrhythmia, and thrombus formation

6 Conclusion

We have reviewed the main principles in our current understanding of how AF affects cardiac biomechanics. We have especially focused on interaction with atrial fibrosis, the presence of which is associated with the occurrence of AF. Interactions between fibrosis and

AF result in negative feedback loops, contributing to progression of both. We then reviewed clinical imaging of atrial fibrosis, in which we first reviewed two MRI-based methods and two methods based on biomechanical properties (i.e., strain and tissue stiffness), as well as 4D flow MRI used for flow imaging. All these methods are also an important source of inputs to computational models, which can be used to decipher underlying mechanisms and potentially as prediction tools. Detecting atrial fibrosis using clinical imaging is also one of the main pathways to providing personalized clinical care to patients. Research on underlying mechanisms, development of clinical imaging techniques, and use of computational models have all proven to be clinically useful in the past, and further development within all these three areas will help clinicians provide better care to their patients.

7 Expert Opinion

Continuous research on fundamental pathophysiology, clinical imaging, and computational modeling can all synergistically contribute to advanced understanding of connections between AF, fibrosis, and thrombogenesis. Clinical images and recordings from wet lab experiments are important inputs to computational models. These can in turn be used to explain underlying mechanisms taking place in the heart as part of an iterative hypothesis testing approach. Additionally, imaging data can reasonably be used directly in clinical settings. Better tools for imaging, segmentation, and interpretation are therefore all key to the development of better, more patient-specific care.

Experimental work in tissue culture, animal models, and with human specimens can provide fundamental understanding of the different pathophysiological subprocesses that take place in disease, especially in the development of fibrosis. Cell- and tissue-level experiments might help us better understand fibrosis-related changes in cells and the surrounding matrix, while stress-strain experiments on cardiac tissue from animal models or humans following heart transplantation might be important for stiffness quantification. Histology studies are also important for understanding structural changes. Further investigation of appropriate classification schemes for the various kinds of fibrosis might be helpful as a means of arriving at more specific diagnoses. Nevertheless, the heterogeneous nature of fibrosis makes this challenging. Deeper understanding of how diffuse fibrosis progresses might translate to clinical tools to prompt reversal of the fibrogenesis process if it can be caught early enough. Experimental work might also support the development of representative biomechanical computational models in quantification of stiffness, relative anisotropy, and structure subject to various degrees of fibrosis.

Clinical imaging is an integral part of patient care. Improvements in imaging techniques and segmentation processes can therefore have near-immediate impact. For LGE-MRI, it would be worth exploring whether specific regional targeting of atrial fibrosis assessment (e.g., within the LAA), could result in more accurate reconstructions of remodeling patterns. Given the sobering variability in results based on different atrial fibrosis quantification techniques, it might be beneficial to coordinate large, multi-center trials in which images acquired in each center are analyzed using the tools and techniques standardized at other institutions. In parallel, this conundrum provides a valuable opportunity to

compare traditional segmentation/analysis techniques to their artificial intelligence-based counterparts. As established in several trials, increased fibrosis is associated with reduced strain, but notably characterization of the latter is less expensive and more accessible compared to the former. As such, potential future directions might involve optimizing strain imaging as a technique complementary to LGE or collecting clinical data serially to assess fibrosis progression over time. T_1 values and elastography techniques fall into a different category of much less explored techniques. They are not likely to be applied clinically in the immediate future but are interesting techniques worthy of further exploration. Further validation with histology would yield incredible valuable information across all imaging techniques as a true baseline, however this is naturally rarely accessible. Combined with emergent tools for high-resolution personalized hemodynamics characterization (e.g., 4D flow MRI), we anticipate that this enriched image-based understanding of atrial structural remodeling will lead to better and more complete understanding of the factors that influence the development and evolution of stroke risk in AF patients.

Multi-scale, multi-physics computational models are emerging as a valuable means of exploring underlying mechanisms and deriving patient-specific insights. One avenue for improving model usefulness is to incorporate multiple imaging techniques and/or new imaging modalities with improved accuracy. LGE and T_1 imaging facilitate direct assessment of fibrosis patterns, while strain and 4D flow MRI can be used for personalization and verification. Elastography could potentially provide relative personalized assessment of cardiac stiffness, which would be valuable for biomechanical model parameterization. Overall, characterization of representative passive properties for atrial myocardium (both healthy and fibrotic) is a major research priority for the field, and a useful avenue for achieving this goal might hybrid experimental/computational studies. Electromechanical models have the potential to improve our common understanding of how AF and atrial fibrosis impairs atrial function. Spatially resolved hemodynamic models could be used to explain how atrial pump, reservoir, and conduit functions are influenced by AF in a patient-specific manner. If combined with information on fibrosis distribution and contractile dysfunction, the synergistic interaction between electrophysiology, biomechanics, and fluid dynamics could be explored with an exquisite level of detail. Data from these models could be further analyzed to understand and predict stroke risk. Finally, making computational simulations fully multi-physics has the potential to shed light on mechanisms from each branch, ultimately revealing new insights on factors underlying the formation of thrombi and ultimately leading to stroke.

We anticipate that segmentation tools for clinical images will soon undergo major improvements, and that many emerging tools and approaches will integrate artificial intelligence in their workflows. We are optimistic that the world's leading researchers in this area will undertake ambitious, large multi-center comparison studies, which we think will yield important insights on how clinical images can best be used in clinical settings. For computational modeling, multi-physics models of varying complexity have recently been developed based on realistic geometries from MRI and CT. In the next five years, we expect that this sub-discipline will continue to develop and flourish, not only by demonstrating the feasibility of running such simulations, but also to apply them in a variety of different clinically interesting research contexts.

Funding:

The work was supported by the following grants: NIH R01-HL160024, NIH R01-HL158667, NIH R01-NS125635, the John Locke Charitable Trust, and the Catherine Holmes Wilkins Charitable Foundation.

Declaration of interest:

The authors have no relevant affiliations or financial involvement with any organization or entity with a financial interest in or financial conflict with the subject matter or materials discussed in the manuscript. This includes employment, consultancies, honoraria, stock ownership or options, expert testimony, grants or patents received or pending, or royalties.

Abbreviations and acronyms:

4D	four-dimensional (3D + time = 4D)
AF	atrial fibrillation
CFD	computational fluid dynamics
CT	computed tomography
ESUS	embolic stroke of undetermined source
ECG	electrocardiogram
IIR	image intensity ratio
LAA	left atrial appendage
LGE	late gadolinium enhancement
MRE	magnetic resonance elastography
MRI	magnetic resonance imaging
PACS	peak atrial contractile strain
PALS	peak atrial longitudinal strain
PIH	pixel intensity histogram
SD	standard deviation(s)
STE	speckle-tracking echocardiography
SWE	shear wave elastography
TDI	tissue doppler imaging
TEE	transesophageal echocardiography

References

1. Kornej J, Börschel CS, Benjamin EJ, Schnabel RB. Epidemiology of Atrial Fibrillation in the 21st Century: Novel Methods and New Insights. *Circ Res*, 127(1), 4–20 (2020). [PubMed: 32716709]

2. van den Ham HA, Klungel OH, Singer DE et al. Comparative Performance of ATRIA, CHADS2, and CHA2DS2-VASc Risk Scores Predicting Stroke in Patients With Atrial Fibrillation: Results From a National Primary Care Database. *J Am Coll Cardiol*, 66(17), 1851–1859 (2015). [PubMed: 26493655]
3. Choi SE, Sagris D, Hill A et al. Atrial fibrillation and stroke. *Expert Rev Cardiovasc Ther*, 21(1), 35–56 (2023). [PubMed: 36537565]
4. Allesie M, Ausma J, Schotten U. Electrical, contractile and structural remodeling during atrial fibrillation. *Cardiovasc Res*, 54(2), 230–246 (2002). [PubMed: 12062329]
5. Yaghi S, Song C, Gray WA et al. Left Atrial Appendage Function and Stroke Risk. *Stroke*, 46(12), 3554–3559 (2015). [PubMed: 26508750]
6. Stojadinovi P, Deshraj A, Wichterle D et al. The hemodynamic effect of simulated atrial fibrillation on left ventricular function. *J Cardiovasc Electrophysiol*, 33(12), 2569–2577 (2022). [PubMed: 36069129]
7. Qiu D, Peng L, Ghista DN, Wong KKL. Left Atrial Remodeling Mechanisms Associated with Atrial Fibrillation. *Cardiovasc Eng Technol*, 12(3), 361–372 (2021). [PubMed: 33650086]
8. Wijesurendra RS, Casadei B. Mechanisms of atrial fibrillation. *Heart*, 105(24), 1860–1867 (2019). [PubMed: 31444267]
9. Honarbakhsh S, Schilling RJ, Orini M et al. Structural remodeling and conduction velocity dynamics in the human left atrium: Relationship with reentrant mechanisms sustaining atrial fibrillation. *Heart Rhythm*, 16(1), 18–25 (2019). [PubMed: 30026014]
10. Liu H, Fan P, Jin F et al. Dynamic and static biomechanical traits of cardiac fibrosis. *Front Bioeng Biotechnol*, 10, 1042030 (2022). [PubMed: 36394025]
11. Wijesurendra RS, Casadei B. Atrial fibrillation: effects beyond the atrium? *Cardiovasc Res*, 105(3), 238–247 (2015). [PubMed: 25587048]
12. Pabel S, Knierim M, Stehle T et al. Effects of Atrial Fibrillation on the Human Ventricle. *Circ Res*, 130(7), 994–1010 (2022). [PubMed: 35193397]
13. Ioannidis P, Zografos T, Christoforatos E et al. The Electrophysiology of Atrial Fibrillation: From Basic Mechanisms to Catheter Ablation. *Cardiol Res Pract*, 2021, 4109269 (2021). [PubMed: 34194824]
14. Kong P, Christia P, Frangogiannis NG. The pathogenesis of cardiac fibrosis. *Cell Mol Life Sci*, 71(4), 549–574 (2014). [PubMed: 23649149]
15. Maruyama K, Imanaka-Yoshida K. The Pathogenesis of Cardiac Fibrosis: A Review of Recent Progress. *Int J Mol Sci*, 23(5), 2617 (2022). [PubMed: 35269759]
16. Yoon M, Yang PS, Jang E et al. Improved Population-Based Clinical Outcomes of Patients with Atrial Fibrillation by Compliance with the Simple ABC (Atrial Fibrillation Better Care) Pathway for Integrated Care Management: A Nationwide Cohort Study. *Thromb Haemost*, 119(10), 1695–1703 (2019). [PubMed: 31266082]
17. Berger WR, Meulendijks ER, Limpens J et al. Persistent atrial fibrillation: A systematic review and meta-analysis of invasive strategies. *Int J Cardiol*, 278, 137–143 (2019). [PubMed: 30553497]
18. Santangeli P, Zado ES, Hutchinson MD et al. Prevalence and distribution of focal triggers in persistent and long-standing persistent atrial fibrillation. *Heart Rhythm*, 13(2), 374–382 (2016). [PubMed: 26477712]
19. Liu T, Xiong F, Qi XY et al. Altered calcium handling produces reentry-promoting action potential alternans in atrial fibrillation-remodeled hearts. *JCI Insight*, 5(8) (2020).
20. Mahnkopf C, Badger TJ, Burgon NS et al. Evaluation of the left atrial substrate in patients with lone atrial fibrillation using delayed-enhanced MRI: implications for disease progression and response to catheter ablation. *Heart Rhythm*, 7(10), 1475–1481 (2010). [PubMed: 20601148]
21. Pellman J, Sheikh F. Atrial fibrillation: mechanisms, therapeutics, and future directions. *Compr Physiol*, 5(2), 649–665 (2015). [PubMed: 25880508]
22. Aliot E, Botto GL, Crijns HJ, Kirchhof P. Quality of life in patients with atrial fibrillation: how to assess it and how to improve it. *Europace*, 16(6), 787–796 (2014). [PubMed: 24469433]
23. Crijns H, Van Gelder IC. Paradigm shifts in pathophysiology and management of atrial fibrillation—a tale of the RACE trials in the Netherlands. *Neth Heart J*, 28(Suppl 1), 3–12 (2020).

24. Santhanakrishnan R, Wang N, Larson MG et al. Atrial Fibrillation Begets Heart Failure and Vice Versa: Temporal Associations and Differences in Preserved Versus Reduced Ejection Fraction. *Circulation*, 133(5), 484–492 (2016). [PubMed: 26746177]
25. Bergau L, Bengel P, Sciacca V et al. Atrial Fibrillation and Heart Failure. *J Clin Med*, 11(9) (2022).
26. Global Burden of Disease 2019 Diseases and Injuries Collaborators. Global burden of 369 diseases and injuries in 204 countries and territories, 1990–2019: a systematic analysis for the Global Burden of Disease Study 2019. *Lancet*, 396(10258), 1204–1222 (2020). [PubMed: 33069326]
27. Adams HP Jr., Bendixen BH, Kappelle LJ et al. Classification of subtype of acute ischemic stroke. Definitions for use in a multicenter clinical trial. TOAST. Trial of Org 10172 in Acute Stroke Treatment. *Stroke*, 24(1), 35–41 (1993). [PubMed: 7678184]
28. White CW, Kerber RE, Weiss HR, Marcus ML. The effects of atrial fibrillation on atrial pressure-volume and flow relationships. *Circ Res*, 51(2), 205–215 (1982). [PubMed: 7094230]
29. Markl M, Lee DC, Furiasse N et al. Left Atrial and Left Atrial Appendage 4D Blood Flow Dynamics in Atrial Fibrillation. *Circ Cardiovasc Imaging*, 9(9), e004984 (2016). [PubMed: 27613699]
30. Gupta KB, Ratcliffe MB, Fallert MA et al. Changes in passive mechanical stiffness of myocardial tissue with aneurysm formation. *Circulation*, 89(5), 2315–2326 (1994). [PubMed: 8181158]
31. Hoit BD. Left atrial size and function: role in prognosis. *J Am Coll Cardiol*, 63(6), 493–505 (2014). [PubMed: 24291276]
32. Yaghi S, Chang A, Ignacio G et al. Left Atrial Appendage Morphology Improves Prediction of Stagnant Flow and Stroke Risk in Atrial Fibrillation. *Circ Arrhythm Electrophysiol*, 13(2), e008074 (2020). [PubMed: 31986073]
33. Dudzi ska-Szczerba K, Kułakowski P, Michałowska I, Baran J. Association Between Left Atrial Appendage Morphology and Function and the Risk of Ischaemic Stroke in Patients with Atrial Fibrillation. *Arrhythm Electrophysiol Rev*, 11, e09 (2022). [PubMed: 35846423]
34. Sajeev JK, Kalman JM, Dewey H et al. The Atrium and Embolic Stroke: Myopathy Not Atrial Fibrillation as the Requisite Determinant? *Jacc-Clin Electrophys*, 6(3), 251–261 (2020).
35. Roka A, Burright I. Remodeling in Persistent Atrial Fibrillation: Pathophysiology and Therapeutic Targets—A Systematic Review. *Physiologia*, 3(1), 43–72 (2023).
36. Denham NC, Pearman CM, Caldwell JL et al. Calcium in the Pathophysiology of Atrial Fibrillation and Heart Failure. *Front Physiol*, 9, 1380 (2018). [PubMed: 30337881]
37. Lugenbiel P, Wenz F, Govorov K et al. Atrial fibrillation complicated by heart failure induces distinct remodeling of calcium cycling proteins. *PLoS One*, 10(3), e0116395 (2015). [PubMed: 25775120]
38. Clarke JD, Caldwell JL, Horn MA et al. Perturbed atrial calcium handling in an ovine model of heart failure: potential roles for reductions in the L-type calcium current. *J Mol Cell Cardiol*, 79, 169–179 (2015). [PubMed: 25463272]
39. Yeh YH, Wakili R, Qi XY et al. Calcium-handling abnormalities underlying atrial arrhythmogenesis and contractile dysfunction in dogs with congestive heart failure. *Circ Arrhythm Electrophysiol*, 1(2), 93–102 (2008). [PubMed: 19808399]
40. Niort BC, Recalde A, Cros C, Brette F. Critical Link between Calcium Regional Heterogeneity and Atrial Fibrillation Susceptibility in Sheep Left Atria. *J Clin Med*, 12(3) (2023).
41. Greiser M, Lederer WJ, Schotten U. Alterations of atrial Ca(2+) handling as cause and consequence of atrial fibrillation. *Cardiovasc Res*, 89(4), 722–733 (2011). [PubMed: 21159669]
42. Schotten U, Greiser M, Benke D et al. Atrial fibrillation-induced atrial contractile dysfunction: a tachycardiomyopathy of a different sort. *Cardiovasc Res*, 53(1), 192–201 (2002). [PubMed: 11744028]
43. Salles S, Espeland T, Molares A et al. 3D Myocardial Mechanical Wave Measurements: Toward In Vivo 3D Myocardial Elasticity Mapping. *JACC Cardiovasc Imaging*, 14(8), 1495–1505 (2021). [PubMed: 32861651]
44. Claridge B, Drack A, Pinto AR, Greening DW. Defining cardiac fibrosis complexity and regulation towards therapeutic development. *Clin Transl Disc*, 3(1), e163 (2023).
45. López B, Ravassa S, Moreno MU et al. Diffuse myocardial fibrosis: mechanisms, diagnosis and therapeutic approaches. *Nat Rev Cardiol*, 18(7), 479–498 (2021). [PubMed: 33568808]

46. Frangogiannis NG. Cardiac fibrosis. *Cardiovasc Res*, 117(6), 1450–1488 (2021). [PubMed: 33135058]
47. Verheule S, Tuyls E, Gharaviri A et al. Loss of continuity in the thin epicardial layer because of endomyocardial fibrosis increases the complexity of atrial fibrillatory conduction. *Circ Arrhythm Electrophysiol*, 6(1), 202–211 (2013). [PubMed: 23390124]
48. Rohr S. Arrhythmogenic implications of fibroblast-myocyte interactions. *Circ Arrhythm Electrophysiol*, 5(2), 442–452 (2012). [PubMed: 22511661]
49. Hanif W, Alex L, Su Y et al. Left atrial remodeling, hypertrophy, and fibrosis in mouse models of heart failure. *Cardiovasc Pathol*, 30, 27–37 (2017). [PubMed: 28759817]
50. Hall C, Gehmlich K, Denning C, Pavlovic D. Complex Relationship Between Cardiac Fibroblasts and Cardiomyocytes in Health and Disease. *J Am Heart Assoc*, 10(5), e019338 (2021). [PubMed: 33586463]
51. Bellini C, Di Martino ES. A mechanical characterization of the porcine atria at the healthy stage and after ventricular tachypacing. *J Biomech Eng*, 134(2), 021008 (2012). [PubMed: 22482675]
52. Richardson WJ, Clarke SA, Quinn TA, Holmes JW. Physiological Implications of Myocardial Scar Structure. *Compr Physiol*, 5(4), 1877–1909 (2015). [PubMed: 26426470]
53. Holmes JW, Nuñez JA, Covell JW. Functional implications of myocardial scar structure. *Am J Physiol*, 272(5 Pt 2), H2123–2130 (1997). [PubMed: 9176277]
54. Sirry MS, Butler JR, Patnaik SS et al. Characterisation of the mechanical properties of infarcted myocardium in the rat under biaxial tension and uniaxial compression. *J Mech Behav Biomed Mater*, 63, 252–264 (2016). [PubMed: 27434651]
55. Mendiola EA, Neelakantan S, Xiang Q et al. Contractile Adaptation of the Left Ventricle Post-myocardial Infarction: Predictions by Rodent-Specific Computational Modeling. *Ann Biomed Eng*, 51(4), 846–863 (2023). [PubMed: 36394778]
56. Fomovsky GM, Holmes JW. Evolution of scar structure, mechanics, and ventricular function after myocardial infarction in the rat. *Am J Physiol Heart Circ Physiol*, 298(1), H221–228 (2010). [PubMed: 19897714]
57. Morita M, Eckert CE, Matsuzaki K et al. Modification of infarct material properties limits adverse ventricular remodeling. *Ann Thorac Surg*, 92(2), 617–624 (2011). [PubMed: 21801916]
58. Johnson RD, Camelliti P. Role of Non-Myocyte Gap Junctions and Connexin Hemichannels in Cardiovascular Health and Disease: Novel Therapeutic Targets? *Int J Mol Sci*, 19(3), 866 (2018). [PubMed: 29543751]
59. Ma J, Chen Q, Ma S. Left atrial fibrosis in atrial fibrillation: Mechanisms, clinical evaluation and management. *J Cell Mol Med*, 25(6), 2764–2775 (2021). [PubMed: 33576189]
60. Li CY, Zhang JR, Hu WN, Li SN. Atrial fibrosis underlying atrial fibrillation (Review). *Int J Mol Med*, 47(3), 1–1 (2021).
61. De Jong AM, Maass AH, Oberdorf-Maass SU et al. Mechanisms of atrial structural changes caused by stretch occurring before and during early atrial fibrillation. *Cardiovasc Res*, 89(4), 754–765 (2011). [PubMed: 21075756]
62. Harada M, Nattel S. Implications of Inflammation and Fibrosis in Atrial Fibrillation Pathophysiology. *Card Electrophysiol Clin*, 13(1), 25–35 (2021). [PubMed: 33516403]
63. Sygitowicz G, Maciejak-Jastrzbska A, Sitkiewicz D. A Review of the Molecular Mechanisms Underlying Cardiac Fibrosis and Atrial Fibrillation. *J Clin Med*, 10(19), 4430 (2021). [PubMed: 34640448]
64. Herum KM, Choppe J, Kumar A et al. Mechanical regulation of cardiac fibroblast profibrotic phenotypes. *Mol Biol Cell*, 28(14), 1871–1882 (2017). [PubMed: 28468977]
65. Egorov YV, Rosenshtraukh LV, Glukhov AV. Arrhythmogenic Interaction Between Sympathetic Tone and Mechanical Stretch in Rat Pulmonary Vein Myocardium. *Front Physiol*, 11, 237 (2020). [PubMed: 32273849]
66. Kalifa J, Jalife J, Zaitsev AV et al. Intra-atrial pressure increases rate and organization of waves emanating from the superior pulmonary veins during atrial fibrillation. *Circulation*, 108(6), 668–671 (2003). [PubMed: 12900337]

67. von Känel R, Kudielka BM, Haerberli A et al. Prothrombotic changes with acute psychological stress: combined effect of hemoconcentration and genuine coagulation activation. *Thromb Res*, 123(4), 622–630 (2009). [PubMed: 18614205]
68. Vita JA, Holbrook M, Palmisano J et al. Flow-induced arterial remodeling relates to endothelial function in the human forearm. *Circulation*, 117(24), 3126–3133 (2008). [PubMed: 18541736]
69. Ward MR, Pasterkamp G, Yeung AC, Borst C. Arterial remodeling. Mechanisms and clinical implications. *Circulation*, 102(10), 1186–1191 (2000). [PubMed: 10973850]
70. Zuo K, Li K, Liu M et al. Correlation of left atrial wall thickness and atrial remodeling in atrial fibrillation: Study based on low-dose-ibutilide-facilitated catheter ablation. *Medicine (Baltimore)*, 98(15), e15170 (2019). [PubMed: 30985700]
71. Vaquero M, Calvo D, Jalife J. Cardiac fibrillation: from ion channels to rotors in the human heart. *Heart Rhythm*, 5(6), 872–879 (2008). [PubMed: 18468960]
72. Beinart R, Khurram IM, Liu S et al. Cardiac magnetic resonance T₁ mapping of left atrial myocardium. *Heart Rhythm*, 10(9), 1325–1331 (2013). [PubMed: 23643513]
73. Ling LH, McLellan AJ, Taylor AJ et al. Magnetic resonance post-contrast T₁ mapping in the human atrium: validation and impact on clinical outcome after catheter ablation for atrial fibrillation. *Heart Rhythm*, 11(9), 1551–1559 (2014). [PubMed: 24931636]
74. Hopman L, Mulder MJ, van der Laan AM et al. Impaired left atrial reservoir and conduit strain in patients with atrial fibrillation and extensive left atrial fibrosis. *J Cardiovasc Magn Reson*, 23(1), 131 (2021). [PubMed: 34758820]
75. Lisi M, Mandoli GE, Cameli M et al. Left atrial strain by speckle tracking predicts atrial fibrosis in patients undergoing heart transplantation. *Eur Heart J Cardiovasc Imaging*, 23(6), 829–835 (2022). [PubMed: 34118154]
76. Çötelci C, Hazırolan T, Aytemir K et al. Evaluation of atrial fibrosis in atrial fibrillation patients with three different methods. *Turk J Med Sci*, 52(1), 175–187 (2022). [PubMed: 34544218] * This article describes a comparison study highlighting how different methods for imaging atrial fibrosis can be used together to gain a deeper understanding of the tissue being examined.
77. Sun BJ, Park JH, Lee M et al. Normal Reference Values for Left Atrial Strain and Its Determinants from a Large Korean Multicenter Registry. *J Cardiovasc Imaging*, 28(3), 186–198 (2020). [PubMed: 32583635]
78. Nielsen AB, Skaarup KG, Djernæs K et al. Left atrial contractile strain predicts recurrence of atrial tachyarrhythmia after catheter ablation. *Int J Cardiol*, 358, 51–57 (2022). [PubMed: 35469934]
79. Siebermair J, Kholmovski EG, Marrouche N. Assessment of Left Atrial Fibrosis by Late Gadolinium Enhancement Magnetic Resonance Imaging: Methodology and Clinical Implications. *Jacc-Clin Electrophys*, 3(8), 791–802 (2017).
80. Harrison JL, Jensen HK, Peel SA et al. Cardiac magnetic resonance and electroanatomical mapping of acute and chronic atrial ablation injury: a histological validation study. *Eur Heart J*, 35(22), 1486–1495 (2014). [PubMed: 24419806]
81. McGann C, Akoum N, Patel A et al. Atrial fibrillation ablation outcome is predicted by left atrial remodeling on MRI. *Circ Arrhythm Electrophysiol*, 7(1), 23–30 (2014). [PubMed: 24363354]
82. Hassan S, Barrett CJ, Crossman DJ. Imaging tools for assessment of myocardial fibrosis in humans: the need for greater detail. *Biophys Rev*, 12(4), 969–987 (2020). [PubMed: 32705483]
83. Menacho K, Ramirez S, Segura P et al. INCA (Peru) Study: Impact of Non-Invasive Cardiac Magnetic Resonance Assessment in the Developing World. *J Am Heart Assoc*, 7(17), e008981 (2018). [PubMed: 30371164]
84. Hopman L, Bhagirath P, Mulder MJ et al. Quantification of left atrial fibrosis by 3D late gadolinium-enhanced cardiac magnetic resonance imaging in patients with atrial fibrillation: impact of different analysis methods. *Eur Heart J Cardiovasc Imaging*, 23(9), 1182–1190 (2022). [PubMed: 35947873] *This article highlights differences in segmentation methods and thresholds for cardiac LGE-MRI. An in-depth discussion of clinical implications is also included.
85. Boyle PM, Sarairah S, Kwan KT et al. Elevated fibrosis burden as assessed by MRI predicts cryoballoon ablation failure. *J Cardiovasc Electrophysiol*, 34(2), 302–312 (2023). [PubMed: 36571158]

86. Marrouche NF, Wilber D, Hindricks G et al. Association of atrial tissue fibrosis identified by delayed enhancement MRI and atrial fibrillation catheter ablation: the DECAAF study. *JAMA*, 311(5), 498–506 (2014). [PubMed: 24496537]
87. Marrouche NF, Wazni O, McGann C et al. Effect of MRI-Guided Fibrosis Ablation vs Conventional Catheter Ablation on Atrial Arrhythmia Recurrence in Patients With Persistent Atrial Fibrillation: The DECAAF II Randomized Clinical Trial. *JAMA*, 327(23), 2296–2305 (2022). [PubMed: 35727277] *This article describes a multi-site, randomized clinical trial in which targeted ablation of LGE-delineated atrial fibrosis was used as an adjunct strategy to pulmonary vein isolation; this did not significantly reduce the rate of post-procedure recurrence in patients with persistent atrial fibrillation.
88. Bisbal F, Benito E, Teis A et al. Magnetic Resonance Imaging-Guided Fibrosis Ablation for the Treatment of Atrial Fibrillation: The ALICIA Trial. *Circ Arrhythm Electrophysiol*, 13(11), e008707 (2020). [PubMed: 33031713]
89. Benito EM, Carlosena-Remirez A, Guasch E et al. Left atrial fibrosis quantification by late gadolinium-enhanced magnetic resonance: a new method to standardize the thresholds for reproducibility. *Europace*, 19(8), 1272–1279 (2017). [PubMed: 27940935]
90. Wu Y, Tang Z, Li B et al. Recent Advances in Fibrosis and Scar Segmentation From Cardiac MRI: A State-of-the-Art Review and Future Perspectives. *Front Physiol*, 12, 709230 (2021). [PubMed: 34413789]
91. Krul SP, Berger WR, Smit NW et al. Atrial fibrosis and conduction slowing in the left atrial appendage of patients undergoing thoracoscopic surgical pulmonary vein isolation for atrial fibrillation. *Circ Arrhythm Electrophysiol*, 8(2), 288–295 (2015). [PubMed: 25673630]
92. Takahashi Y, Yamaguchi T, Otsubo T et al. Histological validation of atrial structural remodelling in patients with atrial fibrillation. *Eur Heart J*, 44(35), 3339–3353 (2023). [PubMed: 37350738]
93. Dekkers IA, Lamb HJ. Clinical application and technical considerations of T(1) & T(2)(*) mapping in cardiac, liver, and renal imaging. *Br J Radiol*, 91(1092), 20170825 (2018). [PubMed: 29975154]
94. Elsafty HG, El Shafey M, El Arabawy R et al. Could native T₁ mapping replace late gadolinium enhancement in the assessment of myocardial fibrosis in patients with cardiomyopathy? *Egypt J Radiol Nucl Med*, 52(1), 222 (2021). *This article compares traditional ventricular late gadolinium enhancement imaging to T₁ mapping, finding that T₁ values capture presence of diffuse fibrosis, which cannot be imaged with using the traditional approach.
95. Bouazizi K, Rahhal A, Kusmia S et al. Differentiation and quantification of fibrosis, fat and fatty fibrosis in human left atrial myocardium using ex vivo MRI. *PLoS One*, 13(10), e0205104 (2018). [PubMed: 30296279]
96. Granitz M, Motloch LJ, Granitz C et al. Comparison of native myocardial T₁ and T₂ mapping at 1.5T and 3T in healthy volunteers : Reference values and clinical implications. *Wien Klin Wochenschr*, 131(7–8), 143–155 (2019). [PubMed: 30519737]
97. Child N, Suna G, Dabir D et al. Comparison of MOLLI, shMOLLI, and SASHA in discrimination between health and disease and relationship with histologically derived collagen volume fraction. *Eur Heart J Cardiovasc Imaging*, 19(7), 768–776 (2018). [PubMed: 29237044]
98. Heidenreich JF, Weng AM, Donhauser J et al. T₁- and ECV-mapping in clinical routine at 3 T: differences between MOLLI, ShMOLLI and SASHA. *BMC Med Imaging*, 19(1), 59 (2019). [PubMed: 31370821]
99. Rauhalaammi SM, Mangion K, Barrientos PH et al. Native myocardial longitudinal (T₁) relaxation time: Regional, age, and sex associations in the healthy adult heart. *J Magn Reson Imaging*, 44(3), 541–548 (2016). [PubMed: 26946323]
100. van den Boomen M, Slart R, Hulleman EV et al. Native T(1) reference values for nonischemic cardiomyopathies and populations with increased cardiovascular risk: A systematic review and meta-analysis. *J Magn Reson Imaging*, 47(4), 891–912 (2018). [PubMed: 29131444]
101. Gottbrecht M, Kramer CM, Salerno M. Native T₁ and Extracellular Volume Measurements by Cardiac MRI in Healthy Adults: A Meta-Analysis. *Radiology*, 290(2), 317–326 (2019). [PubMed: 30422092]

102. Cau R, Bassareo P, Suri JS et al. The emerging role of atrial strain assessed by cardiac MRI in different cardiovascular settings: an up-to-date review. *Eur Radiol*, 32(7), 4384–4394 (2022). [PubMed: 35451607]
103. Kuppahally SS, Akoum N, Burgon NS et al. Left atrial strain and strain rate in patients with paroxysmal and persistent atrial fibrillation: relationship to left atrial structural remodeling detected by delayed-enhancement MRI. *Circ Cardiovasc Imaging*, 3(3), 231–239 (2010). [PubMed: 20133512]
104. Kim J, Park SJ, Jeong DS et al. Left atrial strain predicts fibrosis of left atrial appendage in patients with atrial fibrillation undergoing totally thoracoscopic ablation. *Front Cardiovasc Med*, 10, 1130372 (2023). [PubMed: 37265565]
105. Smiseth OA, Torp H, Opdahl A et al. Myocardial strain imaging: how useful is it in clinical decision making? *Eur Heart J*, 37(15), 1196–1207 (2016). [PubMed: 26508168]
106. Scatteia A, Baritussio A, Bucciarelli-Ducci C. Strain imaging using cardiac magnetic resonance. *Heart Fail Rev*, 22(4), 465–476 (2017). [PubMed: 28620745]
107. Gan GCH, Ferkh A, Boyd A, Thomas L. Left atrial function: evaluation by strain analysis. *Cardiovasc Diagn Ther*, 8(1), 29–46 (2018). [PubMed: 29541609]
108. Qu YY, Buckert D, Ma GS, Rasche V. Quantitative Assessment of Left and Right Atrial Strains Using Cardiovascular Magnetic Resonance Based Tissue Tracking. *Front Cardiovasc Med*, 8, 690240 (2021). [PubMed: 34250043]
109. Caixal G, Alarcón F, Althoff TF et al. Accuracy of left atrial fibrosis detection with cardiac magnetic resonance: correlation of late gadolinium enhancement with endocardial voltage and conduction velocity. *Europace*, 23(3), 380–388 (2021). [PubMed: 33227129]
110. Doyley MM, Parker KJ. Elastography: general principles and clinical applications. *Ultrasound Clin*, 9(1), 1–11 (2014). [PubMed: 24459461]
111. Correia ETO, Barbeta L, Silva O, Mesquita ET. Left Atrial Stiffness: A Predictor of Atrial Fibrillation Recurrence after Radiofrequency Catheter Ablation - A Systematic Review and Meta-Analysis. *Arq Bras Cardiol*, 112(5), 501–508 (2019). [PubMed: 30843918]
112. Villalobos Lizardi JC, Baranger J, Nguyen MB et al. A guide for assessment of myocardial stiffness in health and disease. *Nat Cardiovasc Res*, 1(1), 8–22 (2022).
113. Khan S, Fakhouri F, Majeed W, Kolipaka A. Cardiovascular magnetic resonance elastography: A review. *NMR Biomed*, 31(10), e3853 (2018). [PubMed: 29193358]
114. Caenen A, Pernot M, Nightingale KR et al. Assessing cardiac stiffness using ultrasound shear wave elastography. *Phys Med Biol*, 67(2) (2022).
115. Arani A, Arunachalam SP, Chang ICY et al. Cardiac MR elastography for quantitative assessment of elevated myocardial stiffness in cardiac amyloidosis. *J Magn Reson Imaging*, 46(5), 1361–1367 (2017). [PubMed: 28236336]
116. Villemain O, Correia M, Mousseaux E et al. Myocardial Stiffness Evaluation Using Noninvasive Shear Wave Imaging in Healthy and Hypertrophic Cardiomyopathic Adults. *JACC Cardiovasc Imaging*, 12(7 Pt 1), 1135–1145 (2019). [PubMed: 29550319]
117. Alan B, Alan S. Evaluation of carotid artery stiffness in patients with coronary artery disease using acoustic radiation force impulse elastography. *Vascular*, 31(3), 564–572 (2023). [PubMed: 35226579]
118. Cvijic M, Bézy S, Petrescu A et al. Interplay of cardiac remodelling and myocardial stiffness in hypertensive heart disease: a shear wave imaging study using high-frame rate echocardiography. *Eur Heart J Cardiovasc Imaging*, 21(6), 664–672 (2020). [PubMed: 31377789]
119. Eyerly SA, Vejdani-Jahromi M, Dumont DM et al. The Evolution of Tissue Stiffness at Radiofrequency Ablation Sites During Lesion Formation and in the Peri-Ablation Period. *J Cardiovasc Electrophysiol*, 26(9), 1009–1018 (2015). [PubMed: 25970142]
120. Kwiecinski W, Provost J, Dubois R et al. Quantitative evaluation of atrial radio frequency ablation using intracardiac shear-wave elastography. *Med Phys*, 41(11), 112901 (2014). [PubMed: 25370668]
121. Iskander-Rizk S, Kruizinga P, van der Steen AFW, van Soest G. Spectroscopic photoacoustic imaging of radiofrequency ablation in the left atrium. *Biomed Opt Express*, 9(3), 1309–1322 (2018). [PubMed: 29541523]

122. Iskander-Rizk S, Kruizinga P, Beurskens R et al. Real-time photoacoustic assessment of radiofrequency ablation lesion formation in the left atrium. *Photoacoustics*, 16, 100150 (2019). [PubMed: 31871891]
123. Kim Y-J, Wolf PD, Bahnson TD. Shear Wave Elastography With Intracardiac Echocardiography Characterizes Atrial Stiffness During Catheter Ablation For Atrial Fibrillation. *Circulation*, 140, A17083 (2019).
124. Sayseng V, Grondin J, Salgaonkar VA et al. Catheter Ablation Lesion Visualization With Intracardiac Strain Imaging in Canines and Humans. *IEEE Trans Ultrason Ferroelectr Freq Control*, 67(9), 1800–1810 (2020). [PubMed: 32305909]
125. Couade M, Pernot M, Messas E et al. In vivo quantitative mapping of myocardial stiffening and transmural anisotropy during the cardiac cycle. *IEEE Trans Med Imaging*, 30(2), 295–305 (2011). [PubMed: 20851788]
126. Mazumder R, Clymer BD, White RD et al. In-vivo waveguide cardiac magnetic resonance elastography. *J Cardiovasc Magn Reson*, 17(S1) (2015).
127. Miller R, Kolipaka A, Nash MP, Young AA. Relative identifiability of anisotropic properties from magnetic resonance elastography. *NMR Biomed*, 31(10), e3848 (2018). [PubMed: 29106765]
128. Pashakhanloo F, Herzka DA, Ashikaga H et al. Myofiber Architecture of the Human Atria as Revealed by Submillimeter Diffusion Tensor Imaging. *Circ Arrhythm Electrophysiol*, 9(4), e004133 (2016). [PubMed: 27071829]
129. The Stroke Prevention in Atrial Fibrillation Investigators Committee on Echocardiography. Transesophageal echocardiographic correlates of thromboembolism in high-risk patients with nonvalvular atrial fibrillation. *Ann Intern Med*, 128(8), 639–647 (1998). [PubMed: 9537937]
130. Goldman ME, Pearce LA, Hart RG et al. Pathophysiologic correlates of thromboembolism in nonvalvular atrial fibrillation: I. Reduced flow velocity in the left atrial appendage (The Stroke Prevention in Atrial Fibrillation [SPAF-III] study). *J Am Soc Echocardiogr*, 12(12), 1080–1087 (1999). [PubMed: 10588784]
131. Lee DC, Markl M, Ng J et al. Three-dimensional left atrial blood flow characteristics in patients with atrial fibrillation assessed by 4D flow CMR. *Eur Heart J Cardiovasc Imaging*, 17(11), 1259–1268 (2016). [PubMed: 26590397]
132. Costello BT, Voskoboinik A, Qadri AM et al. Measuring atrial stasis during sinus rhythm in patients with paroxysmal atrial fibrillation using 4 Dimensional flow imaging: 4D flow imaging of atrial stasis. *Int J Cardiol*, 315, 45–50 (2020). [PubMed: 32439367] * This article uses 4D flow magnetic resonance imaging to the important potential role it can play in patient-specific characterization of thromboembolic risk.
133. Ng J, Markl M, Lee DC et al. Structural remodeling determinants of reduced left atrial blood flow measured by 4D flow MRI in patients with atrial fibrillation. *Circulation*, 130(suppl_2), A15673 (2014).
134. van Ooij P, Allen BD, Contaldi C et al. 4D flow MRI and T₁-Mapping: Assessment of altered cardiac hemodynamics and extracellular volume fraction in hypertrophic cardiomyopathy. *J Magn Reson Imaging*, 43(1), 107–114 (2016). [PubMed: 26227419]
135. Blanken CPS, Farag ES, Boekholdt SM et al. Advanced cardiac MRI techniques for evaluation of left-sided valvular heart disease. *J Magn Reson Imaging*, 48(2), 318–329 (2018). [PubMed: 30134000]
136. Dyverfeldt P, Bissell M, Barker AJ et al. 4D flow cardiovascular magnetic resonance consensus statement. *J Cardiovasc Magn Reson*, 17(1), 72 (2015). [PubMed: 26257141]
137. Bissell MM, Raimondi F, Ait Ali L et al. 4D Flow cardiovascular magnetic resonance consensus statement: 2023 update. *J Cardiovasc Magn Reson*, 25(1), 40 (2023). [PubMed: 37474977]
138. Heijman J, Sutanto H, Crijns H et al. Computational models of atrial fibrillation: achievements, challenges, and perspectives for improving clinical care. *Cardiovasc Res*, 117(7), 1682–1699 (2021). [PubMed: 33890620]
139. Niederer SA, Lumens J, Trayanova NA. Computational models in cardiology. *Nat Rev Cardiol*, 16(2), 100–111 (2019). [PubMed: 30361497]
140. Fletcher AG, Osborne JM. Seven challenges in the multiscale modeling of multicellular tissues. *WIREs Mech Dis*, 14(1), e1527 (2022). [PubMed: 35023326]

141. Beheshti M, Umapathy K, Krishnan S. Electrophysiological Cardiac Modeling: A Review. *Crit Rev Biomed Eng*, 44(1–2), 99–122 (2016). [PubMed: 27652454]
142. Clayton RH, Aboelkassem Y, Cantwell CD et al. An audit of uncertainty in multi-scale cardiac electrophysiology models. *Philos Trans A Math Phys Eng Sci*, 378(2173), 20190335 (2020). [PubMed: 32448070]
143. Trayanova NA, Rice JJ. Cardiac electromechanical models: from cell to organ. *Front Physiol*, 2, 43 (2011). [PubMed: 21886622]
144. Quarteroni A, Lassila T, Rossi S, Ruiz-Baier R. Integrated Heart—Coupling multiscale and multiphysics models for the simulation of the cardiac function. *Comput Method Appl M*, 314, 345–407 (2017).
145. Avazmohammadi R, Soares JS, Li DS et al. A Contemporary Look at Biomechanical Models of Myocardium. *Annu Rev Biomed Eng*, 21, 417–442 (2019). [PubMed: 31167105]
146. Hirschhorn M, Tchanchaleishvili V, Stevens R et al. Fluid-structure interaction modeling in cardiovascular medicine - A systematic review 2017–2019. *Med Eng Phys*, 78, 1–13 (2020). [PubMed: 32081559]
147. Morris PD, Narracott A, von Tengg-Kobligk H et al. Computational fluid dynamics modelling in cardiovascular medicine. *Heart*, 102(1), 18–28 (2016). [PubMed: 26512019]
148. Lim CW, Su Y, Yeo SY et al. Automatic 4D reconstruction of patient-specific cardiac mesh with 1-to-1 vertex correspondence from segmented contours lines. *PLoS One*, 9(4), e93747 (2014). [PubMed: 24743555]
149. Razeghi O, Solís-Lemus JA, Lee AWC et al. CemrgApp: An interactive medical imaging application with image processing, computer vision, and machine learning toolkits for cardiovascular research. *SoftwareX*, 12, 100570 (2020). [PubMed: 34124331]
150. Vadakkumpadan F, Rantner LJ, Tice B et al. Image-based models of cardiac structure with applications in arrhythmia and defibrillation studies. *J Electrocardiol*, 42(2), 157 e151–110 (2009).
151. Ackerman MJ. The Visible Human Project. *Proc IEEE*, 86, 504–511 (1998).
152. Sachse FB. Modeling the anatomy of the human heart using the cryosection images of the Visible Female dataset. The third visible human project conference proceedings, (2000).
153. Vigmond EJ, Clements C, McQueen DM, Peskin CS. Effect of bundle branch block on cardiac output: a whole heart simulation study. *Prog Biophys Mol Biol*, 97(2–3), 520–542 (2008). [PubMed: 18384847]
154. Zahid S, Cochet H, Boyle PM et al. Patient-derived models link re-entrant driver localization in atrial fibrillation to fibrosis spatial pattern. *Cardiovasc Res*, 110(3), 443–454 (2016). [PubMed: 27056895]
155. Zhao J, Hansen BJ, Wang Y et al. Three-dimensional Integrated Functional, Structural, and Computational Mapping to Define the Structural “Fingerprints” of Heart-Specific Atrial Fibrillation Drivers in Human Heart Ex Vivo. *J Am Heart Assoc*, 6(8) (2017).
156. Strocchi M, Augustin CM, Gsell MAF et al. A publicly available virtual cohort of four-chamber heart meshes for cardiac electro-mechanics simulations. *PLoS One*, 15(6), e0235145 (2020). [PubMed: 32589679]
157. Fastl TE, Tobon-Gomez C, Crozier A et al. Personalized computational modeling of left atrial geometry and transmural myofiber architecture. *Med Image Anal*, 47, 180–190 (2018). [PubMed: 29753182]
158. Hoermann JM, Pfaller MR, Avena L et al. Automatic mapping of atrial fiber orientations for patient-specific modeling of cardiac electromechanics using image registration. *Int J Numer Method Biomed Eng*, 35(6), e3190 (2019). [PubMed: 30829001]
159. Roney CH, Bendikas R, Pashakhanloo F et al. Constructing a Human Atrial Fibre Atlas. *Ann Biomed Eng*, 49(1), 233–250 (2021). [PubMed: 32458222]
160. Azzolin L, Eichenlaub M, Nagel C et al. AugmentA: Patient-specific augmented atrial model generation tool. *Comput Med Imaging Graph*, 108, 102265 (2023). [PubMed: 37392493]
161. Hunter RJ, Liu Y, Lu Y et al. Left atrial wall stress distribution and its relationship to electrophysiologic remodeling in persistent atrial fibrillation. *Circ Arrhythm Electrophysiol*, 5(2), 351–360 (2012). [PubMed: 22294615]

162. Fritz T, Wieners C, Seemann G et al. Simulation of the contraction of the ventricles in a human heart model including atria and pericardium. *Biomech Model Mechanobiol*, 13(3), 627–641 (2014). [PubMed: 23990017]
163. Augustin CM, Neic A, Liebmann M et al. Anatomically accurate high resolution modeling of human whole heart electromechanics: A strongly scalable algebraic multigrid solver method for nonlinear deformation. *J Comput Phys*, 305, 622–646 (2016). [PubMed: 26819483]
164. Hörmann JM, Bertoglio C, Nagler A et al. Multiphysics Modeling of the Atrial Systole under Standard Ablation Strategies. *Cardiovasc Eng Technol*, 8(2), 205–218 (2017). [PubMed: 28512679]
165. Feng L, Gao H, Griffith B et al. Analysis of a coupled fluid-structure interaction model of the left atrium and mitral valve. *Int J Numer Method Biomed Eng*, 35(11), e3254 (2019). [PubMed: 31454470]
166. Santiago A, Aguado-Sierra J, Zavala-Aké M et al. Fully coupled fluid-electro-mechanical model of the human heart for supercomputers. *Int J Numer Method Biomed Eng*, 34(12), e3140 (2018). [PubMed: 30117302]
167. Augustin CM, Fastl TE, Neic A et al. The impact of wall thickness and curvature on wall stress in patient-specific electromechanical models of the left atrium. *Biomech Model Mechanobiol*, 19(3), 1015–1034 (2020). [PubMed: 31802292]
168. Gerach T, Schuler S, Fröhlich J et al. Electro-Mechanical Whole-Heart Digital Twins: A Fully Coupled Multi-Physics Approach. *Mathematics-Basel*, 9(11), 1247 (2021).
169. Moss R, Wülfers EM, Schuler S et al. A Fully-Coupled Electro-Mechanical Whole-Heart Computational Model: Influence of Cardiac Contraction on the ECG. *Front Physiol*, 12, 778872 (2021). [PubMed: 34975532]
170. Gerach T, Schuler S, Wachter A, Loewe A. The Impact of Standard Ablation Strategies for Atrial Fibrillation on Cardiovascular Performance in a Four-Chamber Heart Model. *Cardiovasc Eng Technol*, 14(2), 296–314 (2023). [PubMed: 36652165]
171. Moyer CB, Norton PT, Ferguson JD, Holmes JW. Changes in Global and Regional Mechanics Due to Atrial Fibrillation: Insights from a Coupled Finite-Element and Circulation Model. *Ann Biomed Eng*, 43(7), 1600–1613 (2015). [PubMed: 25631205]
172. Paliwal N, Ali RL, Salvador M et al. Presence of Left Atrial Fibrosis May Contribute to Aberrant Hemodynamics and Increased Risk of Stroke in Atrial Fibrillation Patients. *Front Physiol*, 12, 657452 (2021). [PubMed: 34163372]
173. Macheret F, Bifulco SF, Scott GD et al. Comparing Inducibility of Reentrant Arrhythmia in Patient-Specific Computational Models to Clinical Atrial Fibrillation Phenotypes. *Jacc-Clin Electrophys*, In press (2023).
174. O’Hara RP, Binka E, Prakosa A et al. Personalized computational heart models with T₁-mapped fibrotic remodeling predict sudden death risk in patients with hypertrophic cardiomyopathy. *Elife*, 11 (2022).
175. Niederer SA, Campbell KS, Campbell SG. A short history of the development of mathematical models of cardiac mechanics. *J Mol Cell Cardiol*, 127, 11–19 (2019). [PubMed: 30503754]
176. Rice JJ, Wang F, Bers DM, de Tombe PP. Approximate model of cooperative activation and crossbridge cycling in cardiac muscle using ordinary differential equations. *Biophys J*, 95(5), 2368–2390 (2008). [PubMed: 18234826]
177. Land S, Niederer SA. A Spatially Detailed Model of Isometric Contraction Based on Competitive Binding of Troponin I Explains Cooperative Interactions between Tropomyosin and Crossbridges. *PLoS Comput Biol*, 11(8), e1004376 (2015). [PubMed: 26262582]
178. Walklate J, Ferrantini C, Johnson CA et al. Alpha and beta myosin isoforms and human atrial and ventricular contraction. *Cell Mol Life Sci*, 78(23), 7309–7337 (2021). [PubMed: 34704115]
179. Prodanovic M, Geeves MA, Poggesi C et al. Effect of Myosin Isoforms on Cardiac Muscle Twitch of Mice, Rats and Humans. *Int J Mol Sci*, 23(3) (2022).
180. Fritz T, Dössel O, Krueger M. Electromechanical Modeling of the Human Atria. *Biomed Tech (Berl)*, 58 Suppl 1(SI-1-Track-N), 000010151520134321 (2013).
181. Brocklehurst P, Ni H, Zhang H, Ye J. Electro-mechanical dynamics of spiral waves in a discrete 2D model of human atrial tissue. *PLoS One*, 12(5), e0176607 (2017). [PubMed: 28510575]

182. Mazhar F, Regazzoni F, Bartolucci C et al. A Novel Human Atrial Electromechanical Cardiomyocyte Model with Mechano-Calcium Feedback Effect. 2022 Computing in Cardiology (2022).
183. Zile MA, Trayanova NA. Increased thin filament activation enhances alternans in human chronic atrial fibrillation. *Am J Physiol Heart Circ Physiol*, 315(5), H1453–H1462 (2018). [PubMed: 30141984]
184. Mazhar F, Bartolucci C, Regazzoni F et al. A detailed mathematical model of the human atrial cardiomyocyte: integration of electrophysiology and cardiomechanics. *J Physiol*, (2023).
185. Narolska NA, Eiras S, van Loon RB et al. Myosin heavy chain composition and the economy of contraction in healthy and diseased human myocardium. *J Muscle Res Cell Motil*, 26(1), 39–48 (2005). [PubMed: 16088376]
186. Adeniran I, MacIver DH, Garratt CJ et al. Effects of Persistent Atrial Fibrillation-Induced Electrical Remodeling on Atrial Electro-Mechanics - Insights from a 3D Model of the Human Atria. *PLoS One*, 10(11), e0142397 (2015). [PubMed: 26606047] *This article describes the use of computational electromechanical modeling to demonstrate independent impact on contractility due to atrial remodeling and rapid pacing.
187. Heikhmakhtiar AK, Tekle AA, Lim KM. Influence of Fibrosis Amount and Patterns on Ventricular Arrhythmogenesis and Pumping Efficacy: Computational Study. *Front Physiol*, 12, 644473 (2021). [PubMed: 34149441]
188. Phung TN, Moyer CB, Norton PT et al. Effect of ablation pattern on mechanical function in the atrium. *Pacing Clin Electrophysiol*, 40(6), 648–654 (2017). [PubMed: 28370137]
189. Palit A, Bhudia SK, Arvanitis TN et al. In vivo estimation of passive biomechanical properties of human myocardium. *Med Biol Eng Comput*, 56(9), 1615–1631 (2018). [PubMed: 29479659]
190. Jernigan SR, Buckner GD, Eischen JW, Cormier DR. Finite element modeling of the left atrium to facilitate the design of an endoscopic atrial retractor. *J Biomech Eng*, 129(6), 825–837 (2007). [PubMed: 18067386]
191. Bellini C, Di Martino ES, Federico S. Mechanical behaviour of the human atria. *Ann Biomed Eng*, 41(7), 1478–1490 (2013). [PubMed: 23263934] *This article presents a mechanical characterization of human atrial tissue, including subregions, fundamental in terms of modeling the passive tension in representative biomechanical atrial or whole-heart models.
192. Javani S, Gordon M, Azadani AN. Biomechanical Properties and Microstructure of Heart Chambers: A Paired Comparison Study in an Ovine Model. *Ann Biomed Eng*, 44(11), 3266–3283 (2016). [PubMed: 27256360]
193. Caggiano LR, Holmes JW. A Comparison of Fiber Based Material Laws for Myocardial Scar. *J Elast*, 145(1–2), 321–337 (2021). [PubMed: 35095176]
194. Martonová D, Alkassar M, Seufert J et al. Passive mechanical properties in healthy and infarcted rat left ventricle characterised via a mixture model. *J Mech Behav Biomed Mater*, 119, 104430 (2021). [PubMed: 33780851]
195. Provost J, Nguyen VT, Legrand D et al. Electromechanical wave imaging for arrhythmias. *Phys Med Biol*, 56(22), L1–11 (2011). [PubMed: 22024555]
196. Grubb CS, Melki L, Wang DY et al. Noninvasive localization of cardiac arrhythmias using electromechanical wave imaging. *Sci Transl Med*, 12(536) (2020).
197. Vagos M, van Herck IGM, Sundnes J et al. Computational Modeling of Electrophysiology and Pharmacotherapy of Atrial Fibrillation: Recent Advances and Future Challenges. *Front Physiol*, 9, 1221 (2018). [PubMed: 30233399]
198. Di Martino ES, Bellini C, Schwartzman DS. In vivo porcine left atrial wall stress: Computational model. *J Biomech*, 44(15), 2589–2594 (2011). [PubMed: 21907340]
199. Ni H, Adeniran I, Zhang H. In-silico investigations of the functional impact of KCNA5 mutations on atrial mechanical dynamics. *J Mol Cell Cardiol*, 111, 86–95 (2017). [PubMed: 28803858]
200. Satriano A, Vigmond EJ, Schwartzman DS, Di Martino ES. Mechano-electric finite element model of the left atrium. *Comput Biol Med*, 96, 24–31 (2018). [PubMed: 29529527]
201. Fedele M, Piersanti R, Regazzoni F et al. A comprehensive and biophysically detailed computational model of the whole human heart electromechanics. *Comput Method Appl M*, 410, 115983 (2023).

202. Viola F, Del Corso G, De Paulis R, Verzicco R. GPU accelerated digital twins of the human heart open new routes for cardiovascular research. *Sci Rep*, 13(1), 8230 (2023). [PubMed: 37217483]
203. Strocchi M, Longobardi S, Augustin CM et al. Cell to whole organ global sensitivity analysis on a four-chamber heart electromechanics model using Gaussian processes emulators. *PLoS Comput Biol*, 19(6), e1011257 (2023). [PubMed: 37363928]
204. Viola F, Meschini V, Verzicco R. Fluid–Structure–Electrophysiology interaction (FSEI) in the left-heart: A multi-way coupled computational model. *Eur J Mech B-Fluid*, 79, 212–232 (2020).
205. Bucelli M, Zingaro A, Africa PC et al. A mathematical model that integrates cardiac electrophysiology, mechanics, and fluid dynamics: Application to the human left heart. *Int J Numer Method Biomed Eng*, 39(3), e3678 (2023). [PubMed: 36579792]
206. Boyle PM, Zghaib T, Zahid S et al. Computationally guided personalized targeted ablation of persistent atrial fibrillation. *Nat Biomed Eng*, 3(11), 870–879 (2019). [PubMed: 31427780]
207. Azzolin L, Eichenlaub M, Nagel C et al. Personalized ablation vs. conventional ablation strategies to terminate atrial fibrillation and prevent recurrence. *Europace*, 25(1), 211–222 (2023). [PubMed: 35943361]
208. Ding WY, Gupta D, Lip GYH. Atrial fibrillation and the prothrombotic state: revisiting Virchow’s triad in 2020. *Heart*, 106(19), 1463–1468 (2020). [PubMed: 32675218]
209. Boyle PM, Del Alamo JC, Akoum N. Fibrosis, atrial fibrillation and stroke: clinical updates and emerging mechanistic models. *Heart*, 107(2), 99–105 (2021). [PubMed: 33097562]
210. Leiderman K, Fogelson A. An overview of mathematical modeling of thrombus formation under flow. *Thromb Res*, 133 Suppl 1, S12–14 (2014). [PubMed: 24759131]
211. Fogelson AL, Neeves KB. Fluid Mechanics of Blood Clot Formation. *Annu Rev Fluid Mech*, 47, 377–403 (2015). [PubMed: 26236058]
212. Qureshi A, Darwish O, Chubb H et al. Modelling Left Atrial Flow and Blood Coagulation for Risk of Thrombus Formation in Atrial Fibrillation. *Comput Cardiol*, (2020).
213. Chen A, Stecker E, Warden BA. Direct Oral Anticoagulant Use: A Practical Guide to Common Clinical Challenges. *J Am Heart Assoc*, 9(13), e017559 (2020). [PubMed: 32538234]
214. Koizumi R, Funamoto K, Hayase T et al. Numerical analysis of hemodynamic changes in the left atrium due to atrial fibrillation. *J Biomech*, 48(3), 472–478 (2015). [PubMed: 25547024]
215. Otani T, Al-Issa A, Pourmorteza A et al. A Computational Framework for Personalized Blood Flow Analysis in the Human Left Atrium. *Ann Biomed Eng*, 44(11), 3284–3294 (2016). [PubMed: 26968855]
216. Masci A, Alessandrini M, Forti D et al. A Proof of Concept for Computational Fluid Dynamic Analysis of the Left Atrium in Atrial Fibrillation on a Patient-Specific Basis. *J Biomech Eng*, 142(1) (2020).
217. Dueñas-Pamplona J, García JG, Sierra-Pallares J et al. A comprehensive comparison of various patient-specific CFD models of the left atrium for atrial fibrillation patients. *Comput Biol Med*, 133, 104423 (2021). [PubMed: 33957460]
218. García-Villalba M, Rossini L, Gonzalo A et al. Demonstration of Patient-Specific Simulations to Assess Left Atrial Appendage Thrombogenesis Risk. *Front Physiol*, 12, 596596 (2021). [PubMed: 33716763] * This article uses computational fluid dynamics modeling of the left atrium to demonstrate that the motion of the wall and the shape of the left atrial appendage make independent contributions to clot formation via prolongation of blood residence times.
219. Gonzalo A, García-Villalba M, Rossini L et al. Non-Newtonian blood rheology impacts left atrial stasis in patient-specific simulations. *Int J Numer Method Biomed Eng*, 38(6), e3597 (2022). [PubMed: 35344280]
220. Mill J, Harrison J, Legghe B et al. In-Silico Analysis of the Influence of Pulmonary Vein Configuration on Left Atrial Haemodynamics and Thrombus Formation in a Large Cohort. In: *Functional Imaging and Modeling of the Heart*. Ennis DB, Perotti LE, Wang VY (Eds.) (Springer International Publishing, 2021)
221. Corti M, Zingaro A, Dede L, Quarteroni AM. Impact of atrial fibrillation on left atrium haemodynamics: A computational fluid dynamics study. *Comput Biol Med*, 150, 106143 (2022). [PubMed: 36182758]

222. Lantz J, Henriksson L, Persson A et al. Patient-Specific Simulation of Cardiac Blood Flow From High-Resolution Computed Tomography. *J Biomech Eng*, 138(12) (2016).
223. Khalili E, Daversin-Catty C, Olivares AL et al. On The Importance of Fundamental Computational Fluid Dynamics Towards a Robust and Reliable Model of Left Atrial Flows: Is There More Than Meets the Eye? arXiv, (2023).
224. Alinezhad L, Ghalichi F, Ahmadelouydarab M, Chenaghloou M. Left atrial appendage shape impacts on the left atrial flow hemodynamics: A numerical hypothesis generating study on two cases. *Comput Methods Programs Biomed*, 213, 106506 (2022). [PubMed: 34752960]
225. Bosi GM, Cook A, Rai R et al. Computational Fluid Dynamic Analysis of the Left Atrial Appendage to Predict Thrombosis Risk. *Front Cardiovasc Med*, 5, 34 (2018). [PubMed: 29670888]
226. Dillon-Murphy D, Marlevi D, Ruijsink B et al. Modeling Left Atrial Flow, Energy, Blood Heating Distribution in Response to Catheter Ablation Therapy. *Front Physiol*, 9, 1757 (2018). [PubMed: 30618785]
227. Dueñas-Pamplona J, García JG, Castro F et al. Morphing the left atrium geometry: A deeper insight into blood stasis within the left atrial appendage. *Applied Mathematical Modelling*, 108, 27–45 (2022).
228. Fang R, Li Y, Zhang Y et al. Impact of left atrial appendage location on risk of thrombus formation in patients with atrial fibrillation. *Biomech Model Mechanobiol*, 20(4), 1431–1443 (2021). [PubMed: 33755847]
229. Fanni BM, Capellini K, Di Leonardo M et al. Correlation between LAA Morphological Features and Computational Fluid Dynamics Analysis for Non-Valvular Atrial Fibrillation Patients. *Appl Sci*, 10, 1448 (2020).
230. Flores O, Rossini L, Gonzalo A et al. Evaluation of Blood Stasis in the Left Atrium Using Patient-Specific Direct Numerical Simulations. In: *Direct and Large Eddy Simulation XII*. García-Villalba M, Kuerten H, Salvetti MV (Eds.) (Springer International Publishing, 2020)
231. García-Isla G, Olivares AL, Silva E et al. Sensitivity analysis of geometrical parameters to study haemodynamics and thrombus formation in the left atrial appendage. *Int J Numer Method Biomed Eng*, e3100 (2018). [PubMed: 29737037]
232. Lantz J, Gupta V, Henriksson L et al. Impact of Pulmonary Venous Inflow on Cardiac Flow Simulations: Comparison with In Vivo 4D Flow MRI. *Ann Biomed Eng*, 47(2), 413–424 (2019). [PubMed: 30362080]
233. Masci A, Barone L, Dede L et al. The Impact of Left Atrium Appendage Morphology on Stroke Risk Assessment in Atrial Fibrillation: A Computational Fluid Dynamics Study. *Front Physiol*, 9, 1938 (2018). [PubMed: 30723422]
234. Sanatkhani S, Nedios S, Menon PG et al. Subject-Specific Calculation of Left Atrial Appendage Blood-Borne Particle Residence Time Distribution in Atrial Fibrillation. *Front Physiol*, 12, 633135 (2021). [PubMed: 34045972]
235. Vella D, Monteleone A, Musotto G et al. Effect of the Alterations in Contractility and Morphology Produced by Atrial Fibrillation on the Thrombosis Potential of the Left Atrial Appendage. *Front Bioeng Biotechnol*, 9, 586041 (2021). [PubMed: 33718333]
236. Wang Y, Qiao YH, Mao YK et al. Numerical prediction of thrombosis risk in left atrium under atrial fibrillation. *Math Biosci Eng*, 17(3), 2348–2360 (2020). [PubMed: 32233539]
237. Tseng AS, Noseworthy PA. Prediction of Atrial Fibrillation Using Machine Learning: A Review. *Front Physiol*, 12, 752317 (2021). [PubMed: 34777014]
238. Chahine Y, Magoon MJ, Maidu B et al. Machine Learning and the Conundrum of Stroke Risk Prediction. *Arrhythm Electrophysiol Rev*, 12, e07 (2023). [PubMed: 37427297]
239. Bifulco SF, Macheret F, Scott GD et al. Explainable Machine Learning to Predict Anchored Reentry Substrate Created by Persistent Atrial Fibrillation Ablation in Computational Models. *J Am Heart Assoc*, 12(16), e030500 (2023). [PubMed: 37581387]
240. Shade JK, Ali RL, Basile D et al. Preprocedure Application of Machine Learning and Mechanistic Simulations Predicts Likelihood of Paroxysmal Atrial Fibrillation Recurrence Following Pulmonary Vein Isolation. *Circ Arrhythm Electrophysiol*, 13(7), e008213 (2020). [PubMed: 32536204]

241. Roney CH, Sim I, Yu J et al. Predicting Atrial Fibrillation Recurrence by Combining Population Data and Virtual Cohorts of Patient-Specific Left Atrial Models. *Circ Arrhythm Electrophysiol*, 15(2), e010253 (2022). [PubMed: 35089057]
242. Carluccio E, Cameli M, Rossi A et al. Left Atrial Strain in the Assessment of Diastolic Function in Heart Failure: A Machine Learning Approach. *Circ Cardiovasc Imaging*, 16(2), e014605 (2023). [PubMed: 36752112]
243. Xiong Z, Xia Q, Hu Z et al. A global benchmark of algorithms for segmenting the left atrium from late gadolinium-enhanced cardiac magnetic resonance imaging. *Med Image Anal*, 67, 101832 (2021). [PubMed: 33166776]
244. Eckstein J, Moghadasi N, Körperich H et al. A Machine Learning Challenge: Detection of Cardiac Amyloidosis Based on Bi-Atrial and Right Ventricular Strain and Cardiac Function. *Diagnostics (Basel)*, 12(11) (2022).
245. Regazzoni F, Salvador M, Dedé L, Quarteroni A. A machine learning method for real-time numerical simulations of cardiac electromechanics. *Comput Methods Appl Mech Eng*, 393, 114825 (2022).
246. Akoum N, Wilber D, Hindricks G et al. MRI Assessment of Ablation-Induced Scarring in Atrial Fibrillation: Analysis from the DECAAF Study. *J Cardiovasc Electrophysiol*, 26(5), 473–480 (2015). [PubMed: 25727106]
247. King JB, Azadani PN, Suksaranjit P et al. Left Atrial Fibrosis and Risk of Cerebrovascular and Cardiovascular Events in Patients With Atrial Fibrillation. *J Am Coll Cardiol*, 70(11), 1311–1321 (2017). [PubMed: 28882227]
248. Parwani AS, Morris DA, Blaschke F et al. Left atrial strain predicts recurrence of atrial arrhythmias after catheter ablation of persistent atrial fibrillation. *Open Heart*, 4(1), e000572 (2017). [PubMed: 28674624]
249. Hopman L, Mulder MJ, van der Laan AM et al. Left atrial strain is associated with arrhythmia recurrence after atrial fibrillation ablation: Cardiac magnetic resonance rapid strain vs. feature tracking strain. *Int J Cardiol*, 378, 23–31 (2023). [PubMed: 36804765]
250. Kurzawski J, Janion-Sadowska A, Zandecki L et al. Global peak left atrial longitudinal strain assessed by transthoracic echocardiography is a good predictor of left atrial appendage thrombus in patients in sinus rhythm with heart failure and very low ejection fraction - an observational study. *Cardiovasc Ultrasound*, 18(1), 7 (2020).
251. Brambatti M, Connolly SJ, Gold MR et al. Temporal relationship between subclinical atrial fibrillation and embolic events. *Circulation*, 129(21), 2094–2099 (2014). [PubMed: 24633881]
252. Tandon K, Tirschwell D, Longstreth WT Jr., et al. Embolic stroke of undetermined source correlates to atrial fibrosis without atrial fibrillation. *Neurology*, 93(4), e381–e387 (2019). [PubMed: 31239359]
253. Kühnlein P, Mahnkopf C, Majersik JJ et al. Atrial fibrosis in embolic stroke of undetermined source: A multicenter study. *Eur J Neurol*, 28(11), 3634–3639 (2021). [PubMed: 34252263]
254. Bifulco SF, Scott GD, Sarairah S et al. Computational modeling identifies embolic stroke of undetermined source patients with potential arrhythmic substrate. *Elife*, 10, e64213 (2021). [PubMed: 33942719] * This article uses electrophysiological models of the human left atrium to explore the possibility that fibrotic remodeling in the hearts of patients with embolic stroke of undetermined source might serve as latent substrate for arrhythmogenic events.
255. Miyauchi S, Tokuyama T, Uotani Y et al. Association between left atrial appendage fibrosis and thrombus formation: A histological approach. *J Cardiovasc Electrophysiol*, 33(4), 677–687 (2022). [PubMed: 35066945]
256. Potpara TS, Lip GYH, Blomstrom-Lundqvist C et al. The 4S-AF Scheme (Stroke Risk; Symptoms; Severity of Burden; Substrate): A Novel Approach to In-Depth Characterization (Rather than Classification) of Atrial Fibrillation. *Thromb Haemost*, 121(3), 270–278 (2021). [PubMed: 32838473]

Article Highlights:

- AF is tightly connected to electrical and structural remodeling, which affects the biomechanical atrial function through various pathways.
- LGE-MRI is the most studied imaging modality for cardiac fibrosis assessment and can serve as an important aid in clinical decision-making. Better image processing tools and use of other imaging techniques, such as T₁ mapping, strain, elastography, and 4D flow MRI are expected to yield additional insights, especially when applied in combination.
- We anticipate that computational models will guide understanding of sub-mechanisms and facilitate quantifications that are not possible to perform with conventional experimental approaches. This will lead to deeper understanding of how AF, atrial fibrosis, and stroke are interconnected. Models are based on atrial geometries and incorporating additional clinical data should be immensely valuable, improving model usefulness and personalization.
- Few multi-physics models of the atria or the whole heart have been developed to date. Biomechanical models can borrow from the more advanced field of electrophysiological modeling, such as considering the same fibrosis patterns, but the need remains for independent experiments to determine biomechanical-specific quantities such as alterations in tissue stiffness and structural anisotropy.
- Augmenting clinical characteristics with advanced imaging and computational tools that are rooted in the mechanisms of arrhythmia, biomechanical, and hemostatic alterations will allow for a more personalized approach to patient care decisions.

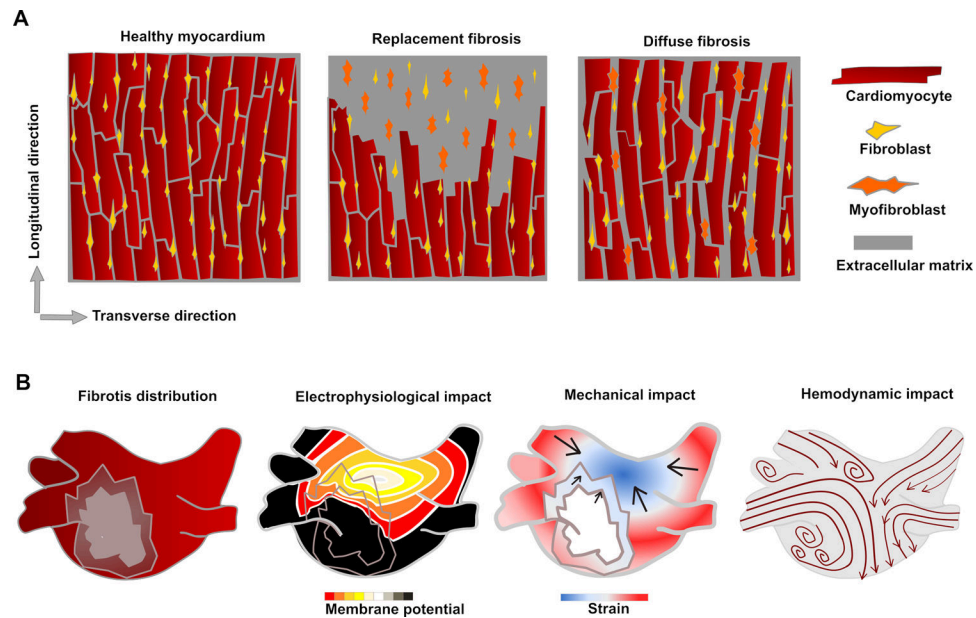


Figure 1: Schematic drawings of fibrotic remodeling on cell-scale and physiological impact on organ-scale. (A) In replacement fibrosis, dead myocytes are replaced with collagenous tissue. In diffuse fibrosis, there is an overproduction of matrix components leading to expansion of interstitial space. In both cases, fibroblast activation leads to accelerated ECM component production. (B) Fibrotic areas in the myocardium have reduced conductivity and reduced or no contractility compared to healthy tissue. The reduced contractility leads to stagnation in the blood flow, which can cause thrombus formation.

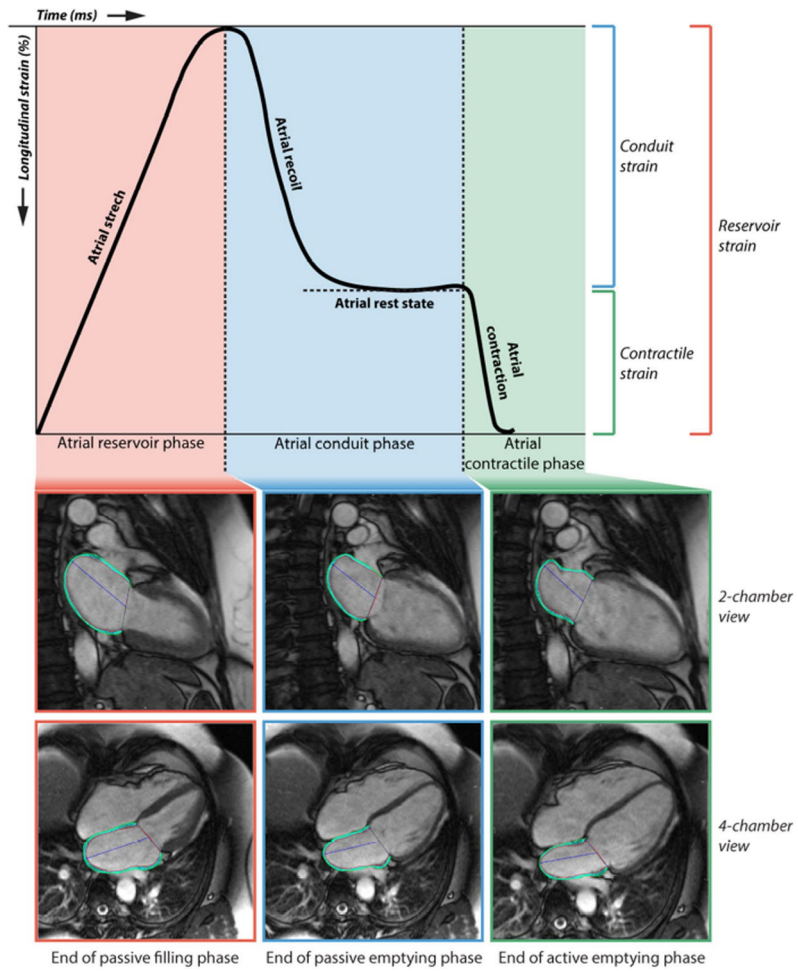


Figure 2: Metrics derived from strain measurement: reservoir, conduit, and contractile strain. Figure originally published in Hopman et al. (2021) [74], distributed under a CC-BY-4.0 license (<https://creativecommons.org/licenses/by/4.0/>).

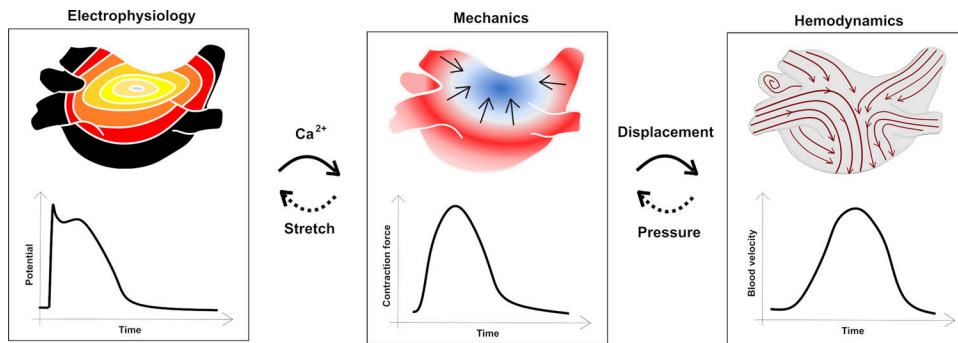


Figure 3: Single-physics computational models and possible connections that make them multi-physics models. Electrophysiological models are connected to biomechanical models through calcium dynamics, which are then linked to hemodynamic models through myocardial wall displacement. Conversely, myocardial stretch impacts electrophysiology and there are fluid-structure interactions wherein blood pressure impacts biomechanics, which is sometimes represented in simulations as feedback mechanisms.

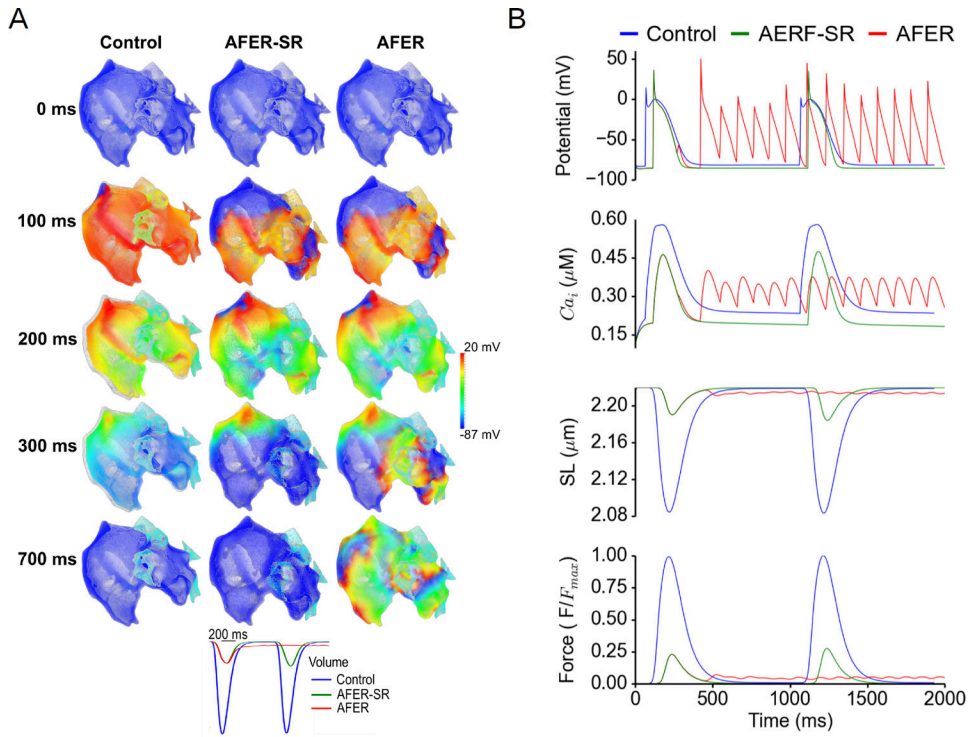


Figure 4:

Results from a computational electromechanical study (Figures 5 and 6 in the original publication [186]) of the human atria. Both sides display a control case compared to AF-induced electrical remodeling (AFER) cases subject to rapid pacing (comparable to AF rates) and in sinus rhythm (-SR), showing the individual contribution of atrial remodeling. (a) Spatial distribution of the electromechanical distribution and displacement at different time shots, superimposed on the original reference configuration as displayed in grey. (b) Average changes in electrical potential, intracellular calcium (Ca_i), sarcomere length (SL), and normalized force. Figure adapted from original figures as distributed in Adeniran et al. (2015) [186], distributed under a CC-BY-4.0 license (<https://creativecommons.org/licenses/by/4.0/>).

Table 1:

Comparison between different possible non-invasive clinical imaging techniques in atrial fibrosis assessment.

Method	Quantification approach	Effect of fibrosis	Reference values*	Advantages	Disadvantages
LGE-MRI	Differences in contrast clearing rates, normalized to healthy myocardium	Delay in contrast clearing rates, higher voxel intensity	N/A	Widely recognized and validated with histological studies, available in many healthcare institutions	Variation in quantification methods leads to different clinical conclusions; not suitable for detection of diffuse fibrosis; somewhat expensive
T₁weighted imaging	Contrast clearing rates (absolute values)	Shorter contrast clearing rates [72,73]	Ling et al. (n=20, 1.5 T) [73], Beinart et al. (n=51, 3.0 T) [72]	Can capture differences in both diffuse and replacement fibrosis, including early remodeling	Few reference values established, somewhat expensive
Strain imaging	Local deformation through numerical differentiation or atrial chamber measurements	Reduced strain, usually assessed via reservoir strain (PALS) and contractile strain (PACS) [74–76]	Sun et al. (n=324) [77], Nielsen et al. (n=1641) [78]	Can quantify contractility over time, potentially real-time, cheaper, and easier to perform routinely	Affected by external factors such as ventricular contraction and blood pressure, sensitive to spatial resolution
Elastography	Material stiffness through tracking reaction to low-frequency vibration	Altered tissue stiffness (mechanical properties)	None yet	Can be used to quantify stiffness changes, makes it possible to differentiate between passive and active tension	No reference values established; requires high image resolution; sensitive to penetration depth, readout complicated by complex atrial myofiber structure, sensitive to spatial resolution

*Reference values for healthy human atrial values; n values refer to the number of healthy control patients enrolled in the cited studies.

Table 2:

Examples of use of clinical data as input to computational biomechanical models of the atria (including electromechanical, mechanofluidic, and multiphysics representations spanning all three branches).

Feature	Input	Significance for/impact on mechanical atrial model	Examples of use
Geometry	MRI, CT	Patient-specific geometrical differences, match of other parameters	[161–169]
Displacement	MRI	Personalization/verification	[170]
Volume/pressure	MRI, CT	Personalization/verification	[161,170,171]
Fibrosis, scar	LGE	Fibrotic patterns; indirect mechanical impact through EP, direct mechanical impact through stiffness and contractility	[172]
Electrical signal	ECG	Verification of the electrophysiological side; indirectly governing active contraction patterns	[169]